

# We are IntechOpen, the world's leading publisher of Open Access books Built by scientists, for scientists

6,900

Open access books available

186,000

International authors and editors

200M

Downloads

Our authors are among the

154

Countries delivered to

TOP 1%

most cited scientists

12.2%

Contributors from top 500 universities



WEB OF SCIENCE™

Selection of our books indexed in the Book Citation Index  
in Web of Science™ Core Collection (BKCI)

Interested in publishing with us?  
Contact [book.department@intechopen.com](mailto:book.department@intechopen.com)

Numbers displayed above are based on latest data collected.  
For more information visit [www.intechopen.com](http://www.intechopen.com)



# Sliding Mode Control of Robot Manipulators via Intelligent Approaches

Seyed Ehsan Shafiei  
Shahrood University of Technology  
Iran

## 1. Introduction

### 1.1 Robot manipulators

Robot manipulators are well-known as nonlinear systems including strong coupling between their dynamics (Craig, 1996). These characteristics, in company with: 1) *structured uncertainties* caused by model imprecision of link parameters, payload variation, etc., and 2) *unstructured uncertainties* produced by un-modeled dynamics –such as nonlinear friction and external disturbances– make the motion control of rigid-link manipulators a complicated problem (Spong & Vidyasagar, 1989). Practice trajectory control is required in many of the sophisticated applications of manipulators (e.g. machining, welding, complex assembly). On the other hand, robot manipulators have to face various uncertainties in their dynamics and they are required to handle various tools and, hence, the dynamic parameters of the robots vary during operation. Thus, it is difficult to initiate an appropriate mathematical model for employing model-based control strategies.

In general, the intelligent control approaches can attenuate the effects of structured parametric uncertainty and unstructured disturbance by using their powerful learning ability without a detailed knowledge of the controlled plant in the design processes. On the other hand, many intelligent control algorithms could have been found for the robot control system without including the actuator dynamics, while, actuator dynamics carry out a significant role in the complete robot dynamics and ignoring them may cause detrimental effects, especially in the case of high-velocity moment, highly varying loads, friction, and actuator saturations (Chang et al., 2008), (Chang & Yen, 2009). Since the electrical actuators are highly controllable in comparison with the other one, they are more convenient for driving manipulators. Also, in practical applications, the voltages or currents of the electrical actuators are accessible for applying control commands and consequently, torque-based control design confronts implementation problems when one intends to apply the torque control commands directly to actuators. Additionally, one constraint in the robot controller designs is saturation nonlinearity of actuators which is less considered in control design of robot manipulators.

### 1.2 Sliding mode control

Sliding mode control (SMC) is a variable-structure, robust control strategy which is capable in controlling different class of uncertain systems including nonlinear systems, MIMO systems, and even discrete time systems (Utkin, 1978), (Zhang et al., 2008). Such

uncertainties may be structured, unstructured, or may result from nondeterministic features of the plant. A sliding mode controller is essentially high gain switching controller. The idea is to keep the trajectory of the system on a particular surface in the phase space. In a two dimensional system this would reduce to following a line in the phase plane. The SMC law is formulated using a Lyapunov approach that guarantees robustness despite the presence of bounded modeling uncertainties (Slotin & Li, 1991).

However, sliding mode control has a good deal of advantages such as insensitivity to parameter variations, disturbance rejection and fast dynamic responses (Zhang et al., 2008). Despite these merits, SMC suffers from some disadvantages. Actually, the sliding mode control law consists of two main parts. The first part is the *equivalent control law* which involves inverse dynamics of model nonlinearities that demonstrates the dependency of SMC on the dynamical model of the plant. The second part is the *robustifying term* which has discontinuous nature and may employ unnecessary high control gain to overcome uncertainties and disturbances. However, this discontinuity may lead to chattering phenomenon that can excite un-modeled high-frequency plant dynamics and harm the overall control system. Also, using high control gain may cause saturating the actuators. Accordingly, several methods have been developed for improving the SMC performance which the most significant of them is intelligent control approach (Kaynak et al., 2001) mainly includes fuzzy logic control and neural network control.

### 1.3 Fuzzy control

Fuzzy control is based on fuzzy logic and is a nonlinear control strategy which uses heuristic information. In the fuzzy control design methodology, human thinking and expert knowledge are incorporated into a fuzzy system that emulates the decision-making process of the human. Basically, a fuzzy system in general or fuzzy control in especial comprises five main parts: 1) fuzzification of inputs, 2) fuzzy control rules, 3) fuzzy implication, 4) fuzzy reasoning and 5) defuzzification (Lee, 1990), (Wang, 1997).

Fuzzy control represents efficient performance in absence of uncertainties and disturbance and where the plant dynamics were well-described with mathematical equations. Moreover, stability of the fuzzy control systems is hard to analyze and needs strong mathematical procedures. Therefore, it seems reasonable to enhance fuzzy control efficiency by using of incorporating well-organized nonlinear control methods (e.g. sliding mode control).

### 1.4 Neural network control

Prominent features of neural networks (NN) have drawn much attention in control research areas especially in robot control systems (Lewis, 1998). Some of this features that are closely related to control design strategies are:

- *Universal approximation*: neural networks can approximate smooth nonlinear functions with any degree of accuracy. This feature may be utilized in nonlinear control systems.
- *Learning and adaptation*: neural networks can be trained off-line with adequate amount of data or they can be adapted on-line with appropriate adaptation laws. This property is applied to identification concerns.
- *MIMO characteristic*: neural networks can accept many inputs and can produce required number of outputs. So they are appropriate for MIMO control systems.

There are many other distinguished features as parallel processing, hardware implementation and data fusion etc. that we neglect them here. Also, fuzzy logic may be employed for constructing special networks like fuzzy-neural-networks. Alternatively, neural networks may be exerted to fuzzy control design like neuro-fuzzy control systems. In the reminder of this chapter three methods are proposed for controller designs. In the first case, sliding mode control plays the main role and fuzzy logic is employed for tuning the controller gains. In the second case, fuzzy control and sliding mode control have the parallel mission in control strategy. Finally, the third case proposes the sliding mode control method by using adaptive neural network approach.

## 2. Sliding mode control using fuzzy approach

### 2.1 Sliding mode PID controller design by using of fuzzy tuning

This section addresses a chattering free sliding mode control (SMC) for a robot manipulator including PID part with a fuzzy tunable gain. The main idea is that the robustness property of SMC and good response characteristics of PID are combined with fuzzy tuning gain approach to achieve more acceptable performance. For this purpose, in the first stage, a PID sliding surface is considered such that the robot dynamical equations can be rewritten in terms of sliding surface and its derivative and the related control law of the SMC design will contain a PID part. The stability guarantee of this sliding mode PID-controller is proved by a lemma using Lyapunov direct method. Then, in the second stage, in order to decrease the reaching time to the sliding surface and deleting the oscillations of the response, a fuzzy tuning system is used for adjusting both controller gains including sliding controller gain parameter and PID coefficients (Ataei & Shafiei, 2008).

#### 2.1.1 Mathematical model of the system

The dynamical equation of an n-link robot manipulator in the standard form is as follows (Spong & Vidyasagar, 1989):

$$M(q)\ddot{q} + C(q, \dot{q})\dot{q} + G(q) + \tau_d = \tau \quad (1)$$

where  $M(q) \in \mathbb{R}^{n \times n}$  is the completed inertia matrix, the vectors  $q, \dot{q}, \ddot{q} \in \mathbb{R}^n$  are the position, velocity and angular acceleration of the robot joints, respectively. Moreover, the matrix  $C(q, \dot{q}) \in \mathbb{R}^{n \times n}$  is the matrix of Coriolis and centrifugal forces and  $G(q) \in \mathbb{R}^n$  is the gravity vector. Also,  $\tau_d \in \mathbb{R}^n$  denotes the vector of disturbance and un-modeled dynamics, and finally,  $\tau$  is the torque vector. In the following, two conventional properties of the robot manipulators are considered.

*Property 2.1.* The inertia matrix  $M(q)$  is symmetric and positive definite,  $M^T = M$ .

*Property 2.2.* The matrix of  $(\dot{M} - 2C)$  is skew-symmetric, i.e. for any vector of  $X$ , we have  $X^T(\dot{M} - 2C)X = 0$ .

#### 2.1.2 Sliding mode control with PID

The objective of the tracking control is to design such a control law, for obtaining the suitable input torque  $\tau$ , that the position vector  $q$  could track the desired trajectory  $q_d$ . In this regard, the tracking error vector is defined as follows:

$$e = q_d - q \quad (2)$$

In order to apply the SMC, the sliding surface is considered as relation (3) which contains the integral part in addition to the derivative term:

$$s = \dot{e} + \lambda_1 e + \lambda_2 \int_0^t e dt \quad (3)$$

where  $\lambda_i$  is diagonal positive definite matrix. Therefore,  $s = 0$  is a stable sliding surface and  $e \rightarrow 0$  as  $t \rightarrow \infty$ . The robot dynamical equations can be rewritten based on the sliding surface (in term of filtered error) as:

$$M\dot{s} = -Cs + f + \tau_d - \tau \quad (4)$$

Where

$$f = M(\ddot{q}_d + \lambda_1 \dot{e} + \lambda_2 e) + C(\dot{q}_d + \lambda_1 e + \lambda_2 \int_0^t e dt) + G \quad (5)$$

Now, the control input can be considered as:

$$\tau = \hat{f} + K_v s + K s \operatorname{sgn}(s) \quad (6)$$

where

$$\hat{f} = \hat{M}(\ddot{q}_d + \lambda_1 \dot{e} + \lambda_2 e) + \hat{C}(\dot{q}_d + \lambda_1 e + \lambda_2 \int_0^t e dt) + \hat{G} \quad (7)$$

is an estimation of  $f$  and  $K_v s = K_v \dot{e} + K_v \lambda e + K_v \lambda \int_0^t e dt$  is the outer PID tracking loop, and  $K_v, K$  are diagonal positive definite matrices and are defined such that the stability conditions are guaranteed. The  $\operatorname{sgn}(s)$  is also the sign function.

We have also:

$$|\tilde{f}| = |\tilde{M}(\ddot{q}_d + \lambda_1 \dot{e} + \lambda_2 e) + \tilde{C}(\dot{q}_d + \lambda_1 e + \lambda_2 \int_0^t e dt) + \tilde{G}| \leq F \quad (8)$$

where  $\tilde{f} = f - \hat{f}$ ,  $\tilde{M} = M - \hat{M}$ ,  $\tilde{C} = C - \hat{C}$ , and  $\tilde{G} = G - \hat{G}$ . Vector  $F$  can also be selected as the following relation:

$$F = |\tilde{M}(\ddot{q}_d + \lambda_1 \dot{e} + \lambda_2 e)| + |\tilde{C}(\dot{q}_d + \lambda_1 e + \lambda_2 \int_0^t e dt)| + |\tilde{G}| \quad (9)$$

In order to govern the system states  $(e, \dot{e})$  to reach the sliding surface  $s = 0$  in a limited time and to remain there, the control law should be designed such that the following sliding condition is satisfied (Slotin & Li, 1991):

$$\frac{1}{2} \frac{d}{dt} [s^T M s] < -\eta (s^T s)^{1/2}, \quad \eta > 0 \quad (10)$$

This aim is fulfilled in the following lemma.

**Lemma 2.1.** In the SMC design of a system with dynamical equation (1) and sliding surface (3), if the control input  $\tau$  is selected as (6), by considering  $F$  as (9) and  $K = \operatorname{diag}(K_{11}, K_{22}, \dots, K_{nn})$  with the following components:

$$K_{ii} = [F + |K_v s| + T_D + \eta]_i, \quad i = 1, 2, \dots, n \quad (11)$$

Then, the sliding condition (10) is satisfied by equation (4).

*Proof.* Consider the following Lyapunov function candidate:

$$V = \frac{1}{2} s^T M s \quad (12)$$

Since  $M$  is positive definite, for  $s \neq 0$  we have  $V > 0$  and by taking derivative from relation (12) and regarding the symmetric property of  $M$ , it can be written:

$$\dot{V} = \frac{1}{2} s^T \dot{M} s + s^T M \dot{s} \quad (13)$$

By substituting (4) into (13) and considering that  $s^T (\dot{M} - 2C)s = 0$ , we have:

$$\dot{V} = \frac{1}{2} s^T \dot{M} s - s^T C s + s^T (f + \tau_d - \tau) = s^T (f + \tau_d - \tau) \quad (14)$$

By replacing the relation (6) into (14),  $\dot{V}$  can be rewritten as:

$$\dot{V} = s^T (f + \tau_d - \hat{f} - K_v s - K \text{sgn}(s)) = s^T (\tilde{f} + \tau_d - K_v s) - \sum_{i=1}^n K_{ii} |s_i| \quad (15)$$

Since the following inequality (16) is valid and by regarding the relation (11), we have:

$$F + |K_v s| + T_D \geq |\tilde{f} + \tau_d - K_v s| \quad (16)$$

$$K_{ii} \geq |[\tilde{f} + \tau_d - K_v s]_i| + \eta_i \quad (17)$$

Finally, it can be concluded that:

$$\dot{V} \leq -\sum_{i=1}^n \eta_i |s_i| \quad (18)$$

This indicates that  $V$  is a Lyapunov function and the sliding condition (10) has been satisfied.

The use of sign function in the control law leads to high oscillations in control torque which is undesired phenomenon and is called chattering. To overcome this drawback, there are some solutions that one of them is using the following saturation function instead of sign function in the discontinuous part of the control law:

$$\text{sat}\left(\frac{s}{\varphi}\right) = \begin{cases} 1 & s \geq \varphi \\ \frac{s}{\varphi} & -\kappa < s < \varphi \\ -1 & s \leq -\varphi \end{cases} \quad (19)$$



By this, there is a boundary layer  $\varphi$  around the sliding surface such that once the state trajectory reaches this layer, then it will be remaining there.

2.1.3 Fuzzy gain tuning

As mentioned before, by using a high gain in SMC, i.e.  $K$ , the sensitivity of the controller to the model uncertainties and external disturbances can be reduced. Moreover, a high gain in PID part of the control system ( $K_v$ ) can reduce the reaching time to sliding surface and tracking error. However, increasing the gain causes the increment of the oscillations in the input torque around the sliding surface. Therefore, if this gain can be tuned based on the distance of the states to the sliding surface, a more acceptable performance can be achieved. In the other words, the value of gain should be selected high when the state trajectory is far from the sliding surface and when the distance is decreasing, its value should be decreased. This idea can be accomplished by using fuzzy logic in combination with SMC to tune the gain adaptively.

For this purpose, two-input one-output fuzzy system is designed whose inputs are  $s$  and  $\dot{s}$  which are the distance of state trajectories to the sliding surface and its derivative, respectively. The membership functions of these two inputs are shown in Fig. 1. The output of the fuzzy system is denoted by  $K_{fuzz}$  and has been shown in Fig. 2. For applying these gains to the control input, the normalization factors  $N$  and  $N_v$  are used as the following relations:

$$K = N \cdot K_{fuzz}$$

(20)

$$K_v = N_v \cdot K_{fuzz}$$

(21)

These factors can be selected by trial and error such that the stability condition (17) is satisfied.

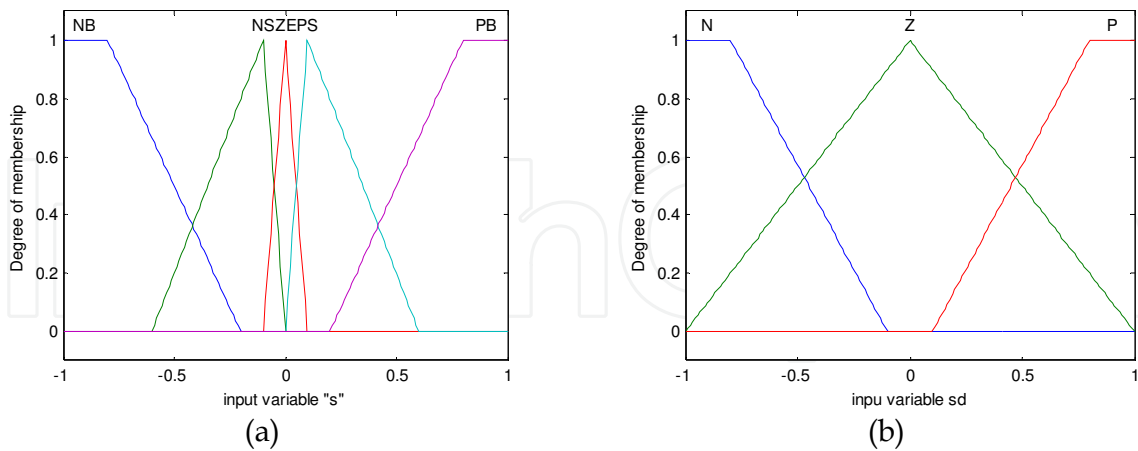


Fig. 1. The membership functions, (a) input  $s$ , (b) input  $\dot{s}$

The maximum values of  $K$  and  $K_v$  are limited according to the system actuators power, and the minimum value of  $K$  should not be less than the provided amount in relation (17). The fuzzy rule base has been given in table 1 in which the following abbreviations have been used: NB: Negative Big; NS: Negative Small; Z: Zero; PS: Positive Small; PB: Positive Big; M: Medium. For example, when  $s$  is negative small (NS) and  $\dot{s}$  is positive (P), then  $K_{fuzz}$  is small (S).

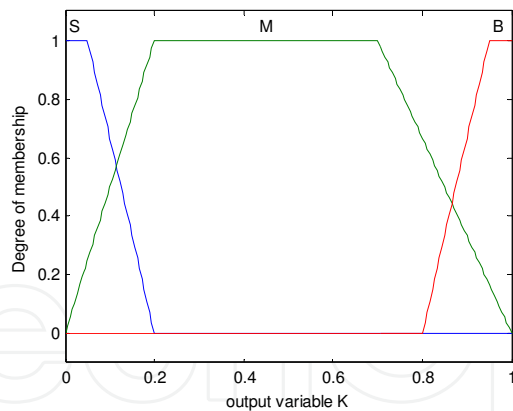


Fig. 2. The membership functions of the output  $K_{fuzz}$

$s \backslash \dot{s}$	NB	NS	Z	PS	PB
N	B	B	M	S	B
Z	B	M	S	M	B
P	B	S	M	B	B

Table 1. The fuzzy rule base for tuning  $K_{fuzz}$

**Simulation example 2.1.** In order to show the effectiveness of the proposed control law, it is applied to a two-link robot with the following parameters:

$$M(q)=\begin{bmatrix} \alpha+\beta+2\gamma\cos q_2 & \beta+\gamma\cos q_2 \\ \beta+\gamma\cos q_2 & \beta \end{bmatrix} \tag{22}$$

$$C(q,\dot{q})=\begin{bmatrix} -\gamma\dot{q}_2\sin q_2 & -\gamma(\dot{q}_1+\dot{q}_2)\sin q_2 \\ \gamma\dot{q}_1\sin q_2 & 0 \end{bmatrix} \tag{23}$$

$$G(q)=\begin{bmatrix} \alpha\delta_1\cos q_1+\gamma\delta_1\cos(q_1+q_2) \\ \gamma\delta_1\cos(q_1+q_2) \end{bmatrix} \tag{24}$$

where  $\alpha=(m_1+m_2)a_1^2$ ,  $\beta=m_2a_2^2$ ,  $\gamma=m_2a_1a_2$ ,  $\delta=g/a_1$ , and  $m_1$ ,  $m_2$ ,  $a_1=.7$ ,  $a_2=.5$  are the masses and lengths of the first and second links, respectively. The masses are assumed to be in the end of the arms and the gravity acceleration is considered as  $g=9.8$ . Moreover, the masses are considered with 10% uncertainty as follow:

$$\begin{aligned} m_1 &= m_{1_0} + \Delta m_1, \quad |\Delta m_1| \leq .4 \\ m_2 &= m_{2_0} + \Delta m_2, \quad |\Delta m_2| \leq .2 \end{aligned} \tag{25}$$

where  $m_{1_0}=4$  and  $m_{2_0}=2$ , and  $\hat{M}$ ,  $\hat{C}$ , and  $\hat{G}$  are estimated. The desired state trajectory is:

$$q_d=\begin{bmatrix} 1-\cos \pi t \\ 2\cos \pi t \end{bmatrix} \tag{26}$$



and the disturbance torque is considered as:

$$\tau_d = \begin{bmatrix} 0.5 \sin 2\pi t \\ 0.5 \sin 2\pi t \end{bmatrix} \quad (27)$$

which leads to  $T_d = \begin{bmatrix} 0.5 \\ 0.5 \end{bmatrix}$ .

The design parameters are determined as follow:

$$\lambda_1 = \begin{bmatrix} 15 & 0 \\ 0 & 15 \end{bmatrix}, \lambda_2 = \begin{bmatrix} 40 & 0 \\ 0 & 40 \end{bmatrix} \quad (28)$$

Values of  $\varphi$  and  $\eta$  are selected as  $\varphi = 0.167$  and  $\eta = [0.1 \ 0.1]^T$ . Moreover, the factors  $N$  and  $N_v$  are selected as:

$$N = \begin{bmatrix} 50 & 0 \\ 0 & 5 \end{bmatrix}, N_v = \begin{bmatrix} 5 & 0 \\ 0 & 10 \end{bmatrix} \quad (29)$$

In order to show the improvement due to the proposed method, the simulation results of applying this method are compared with the related results of the conventional SMC. The tracking error and control law in the case of conventional SMC have been shown in Fig. 3 and Fig. 4, respectively. The corresponding graphs for the case of applying fuzzy SMC-PID are also provided in Fig. 5 and 6.

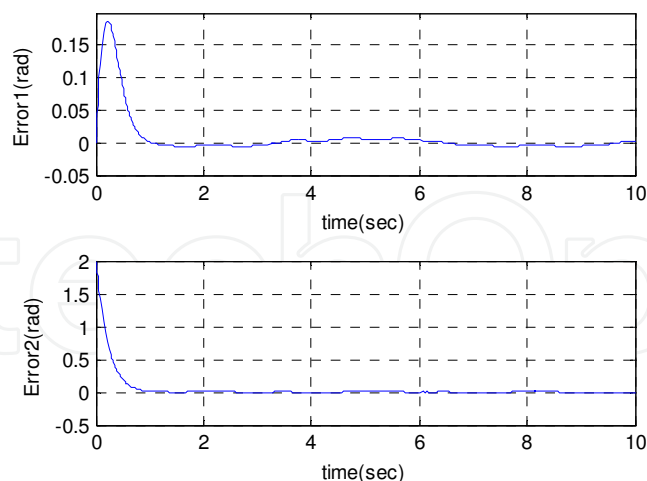


Fig. 3. The tracking errors in the case of using conventional SMC

As it can be seen from these figures, the proposed fuzzy SMC-PID has faster response and less tracking error in comparison with conventional SMC. In order to show more clearly the difference between the tracking errors in two cases, the enlarged graphs have been provided in Fig. 7 and 8.

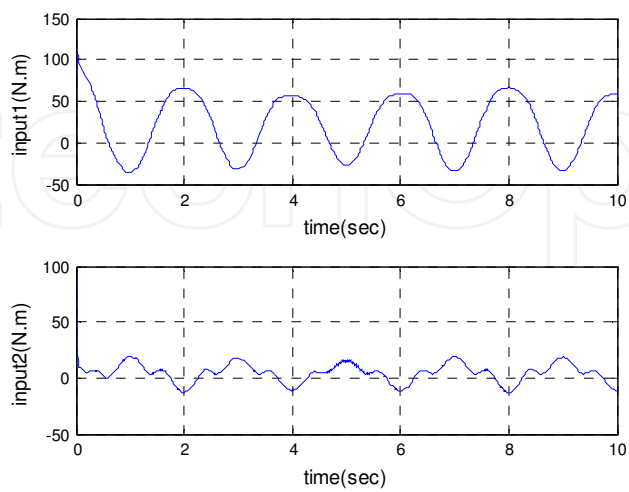


Fig. 4. The control inputs in the case of using conventional SMC

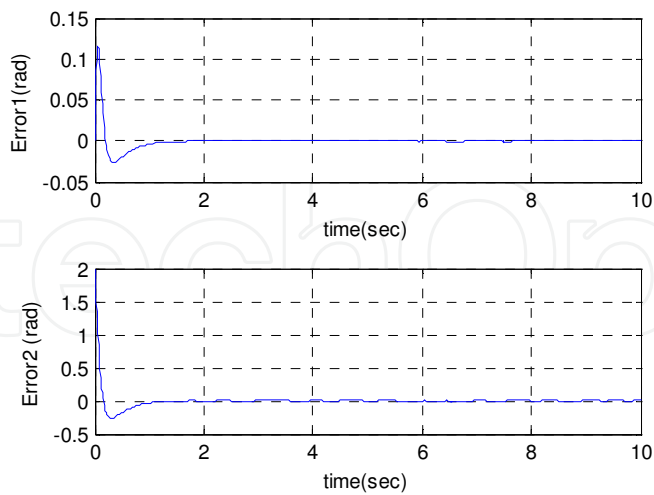


Fig. 5. The tracking errors in the case of using Fuzzy SMC-PID

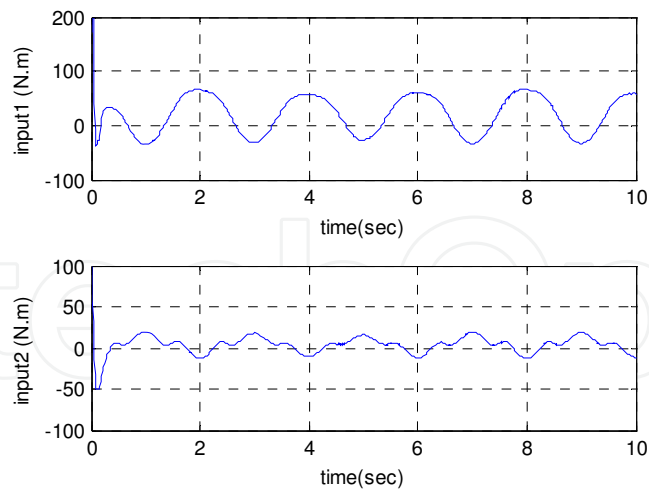


Fig. 6. The control inputs in the case of using Fuzzy SMC-PID

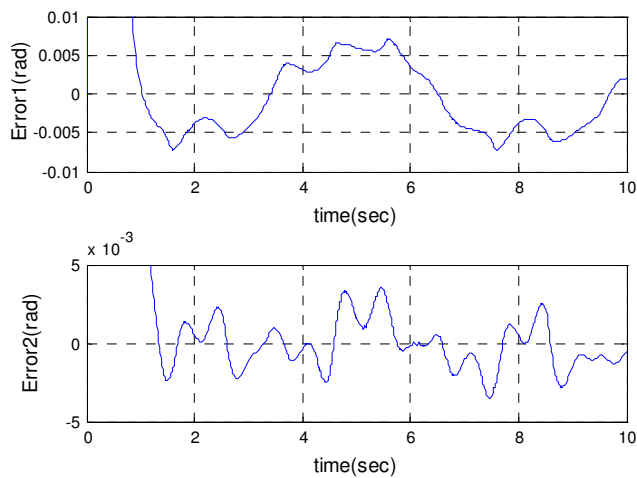


Fig. 7. The enlargement of the tracking errors in the case of using conventional SMC

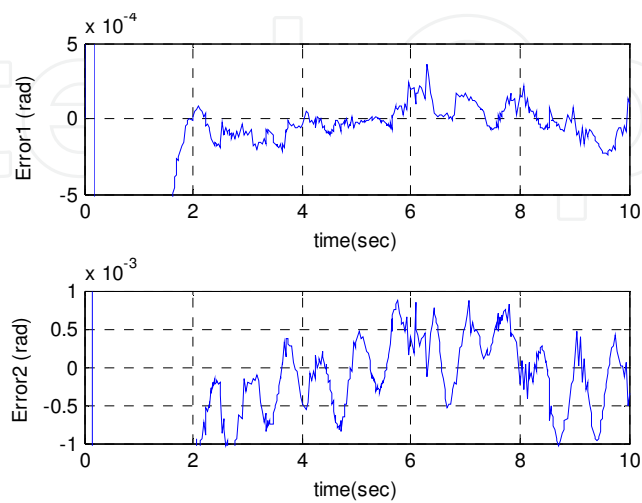


Fig. 8. The enlargement of the tracking errors in the case of using Fuzzy SMC-PID

## 2.2 Incorporating sliding mode and fuzzy control

In this section, a combined controller includes SMC term and fuzzy term is proposed for set-point tracking of robot manipulators. Some practical issues, such as existence of joint frictions, restriction on input torque magnitude due to saturation of actuators, and modeling uncertainties have been considered here. Design procedure contains two steps. First, SMC design is accomplished and system stability in this case is provided by Lyapunov direct method. When the tracking error would be less than predefined value then a sectorial fuzzy controller (SFC), (Calcev, 1998), is responsible for control action. Designing of this kind of fuzzy controller is exactly the same as in which has performed in (Santibanez et al., 2005).

This proposed controller has following advantages. 1) There are less tracking errors versus traditional SMC in condition that the control input is limited, 2) the chattering is avoided, 3) convergence of tracking error is more rapid than fuzzy controller designed in (Santibanez et al., 2005) and modeling uncertainty is considered here (Shafiei & Sepasi, 2010).

### 2.2.1 Mathematical model and problem formulation

This time the friction of joint is considered and is added to dynamical equation (1) as:

$$M(q)\ddot{q} + C(q, \dot{q})\dot{q} + G(q) + F(\dot{q}, \tau) = \tau \quad (30)$$

where  $F(\dot{q}, \tau) \in R^n$  stands for the friction vector which is as follows (Cai & Song, 1994):

$$f_i(\dot{q}, \tau_i) = b_i \dot{q}_i + f_{ci} \operatorname{sgn}(\dot{q}_i) + [1 - |\operatorname{sgn}(\dot{q}_i)|] \operatorname{sat}(\tau_i; f_{si}) \quad (31)$$

where  $f_i(\dot{q}, \tau_i)$ ,  $i = 1, 2, \dots, n$ , denotes the  $i$ -th element of  $F(\dot{q}, \tau)$  vector.  $b_i$ ,  $f_{ci}$  and  $f_{si}$  are the viscous, Coulomb and static friction, respectively. The  $\operatorname{sat}(\cdot; \cdot)$  indicates saturation function with following equation.

$$\operatorname{sat}(x; r) = \begin{cases} r & \text{if } x > r \\ x & \text{if } -r \leq x \leq r \\ -r & \text{if } x < -r \end{cases}$$

In the following,  $M(q)$ ,  $C(q, \dot{q})$  and  $G(q)$  might be shown by  $M$ ,  $C$ , and  $G$ , respectively in where it would be requisite.

Now, the boundedness properties are defined as below:

$$\sup_{q \in R^n} \{ |g_i(q)| \} \leq \bar{g}_i, \quad i = 1, \dots, n \quad (32)$$

where  $g_i$  stands for the  $i$ -th element of  $G(q)$  and  $\bar{g}_i$  is finite nonnegative constant. Assume that the maximum torque that joint actuator can supply is  $\tau^{\max}$ . Therefore:

$$|\tau_i| \leq \tau_i^{\max}, \quad i = 1, \dots, n \quad (33)$$

and each actuator satisfies the following condition:

$$\tau_i^{\max} > \bar{g}_i + f_{si} \quad (34)$$

In robot modeling, one can well determine the terms  $M(q)$  and  $G(q)$  but it is difficult in most cases obtaining the parameters of  $C(q, \dot{q})$  and  $F(\dot{q}, \tau)$  exactly. So, in present section, the matrix  $C$  is considered as follows:

$$C = \hat{C} + \Delta C \quad (35)$$

where  $\hat{C}$  denotes estimation of  $C$ , and  $\Delta C$  is bounded estimation error which has the following relation:

$$|\Delta C_{i,j}| \leq 0.1 |C_{i,j}| \quad (36)$$

where  $C_{i,j}$  stands for elements of the matrix  $C$ . Also the vector  $F$  is supposed as an external disturbance with the following unknown upper bound:

$$\|F\| \leq F_{up} \quad (37)$$

where the operator  $\|\cdot\|$  denotes Euclidean norm.

If one considers the desired point which joint position must be held on it as  $q_d$ , then the position error could be defined as:

$$\tilde{q} = q_d - q \quad (38)$$

Here, the set-point tracking problem refers to define the control law such that error  $e$  would be driven toward the inside of an arbitrary small region around zero with maintaining the torques within the constraints (33). In succeeding subsections, this aim will be attained.

### 2.2.2 Sliding mode controller design

The following sliding surface is considered for designing SMC controller.

$$s = \dot{e} + \lambda e \quad (39)$$

where  $e = -\tilde{q} = q - q_d$  is error vector and  $\lambda$  is supposed symmetric positive definite matrix such that  $s=0$  would become a stable surface. The reference velocity vector " $\dot{q}_r$ " is defined as in (Slotin & Li, 1991):

$$\dot{q}_r = \dot{q}_d - \lambda e \quad (40)$$

Thus, one can interpret sliding surface as:

$$s = \dot{q} - \dot{q}_r \quad (41)$$

Here, the SMC controller design is expressed by lemma 2.2.

**Lemma 2.2.** Consider the system with dynamic equation (30) and sliding surface and reference velocity defined by (39) and (40), respectively. If one chooses the control law below,

$$\tau = \hat{\tau} - K \text{sgn}(s) \quad (42)$$

such that

$$\hat{\tau} = M\ddot{q}_r + \hat{C}\dot{q}_r + G \quad (43)$$

and

$$K_i \geq \|\Delta C\dot{q}_r\| + \Gamma_i \quad (44)$$

then the sliding condition (10) is satisfied. In the last inequality,  $K_i$  denotes the element of sliding gain vector  $K$  and  $\Gamma$  is design parameter vector which must be selected such that  $\Gamma_i \geq F_{up} + \eta_i$ .

*Proof.* Consider the following Lyapunov function candidate:

$$V = \frac{1}{2} s^T M s \quad (45)$$

Since  $M$  is positive definite, for  $s \neq 0$  we have  $V > 0$  and by taking time derivative of the relation (45) and regarding the symmetric property of  $M$ , it can be written:

$$\dot{V} = s^T M \dot{s} + \frac{1}{2} s^T \dot{M} s \quad (46)$$

from (40), gives:

$$\dot{V} = s^T (M\ddot{q} - M\ddot{q}_r) + \frac{1}{2} s^T \dot{M} s \quad (47)$$

By substituting (30) in (47) and considering asymmetry property  $s^T (\dot{M} - 2C)s = 0$ , we have:

$$\dot{V} = s^T (\tau - C\dot{q}_r - G - F - M\ddot{q}_r) \quad (48)$$

Now, applying (42) and (43) yields:

$$\dot{V} = s^T (\Delta C\dot{q}_r + F) - \sum_{i=1}^n K_i |s_i| \quad (49)$$

Finally, from relation (44) it can be concluded that:

$$\dot{V} \leq -\sum_{i=1}^n \eta_i |s_i| \quad (50)$$

This indicates that  $V$  is a Lyapunov function and the sliding condition (10) has been satisfied.

Note that, in general, the sign function is replaced by saturation function as  $\text{sat}(s/\varphi)$ , where  $\varphi$  denotes boundary layer thickness.

### 2.2.3 Fuzzy controller design

In this section, the SFC class of fuzzy controller studied in (Santibanez et al., 2005) is considered which has two-input one-output rules used in the formulation of the knowledge base. These IF-THEN rules have following form:

$$\text{IF } x_1 \text{ is } A_1^{l_1} \text{ and } x_2 \text{ is } A_2^{l_2} \text{ THEN } y \text{ is } B^{l_2}$$

(51)

where  $x = [x_1 \ x_2]^T \in U = U_1 \times U_2 \subset \mathbb{R}^2$  and  $y \in V \subset \mathbb{R}$ . For each input fuzzy set  $A_j^{l_j}$  in  $x_j \subset U_j$  and output fuzzy set  $B^{l_2}$  in  $y \subset V$ , exist an input membership function  $\mu_{A_j^{l_j}}(x_j)$  and output membership function  $\mu_{B^{l_2}}(y)$  shown in Fig. 10 and Fig. 11, respectively.

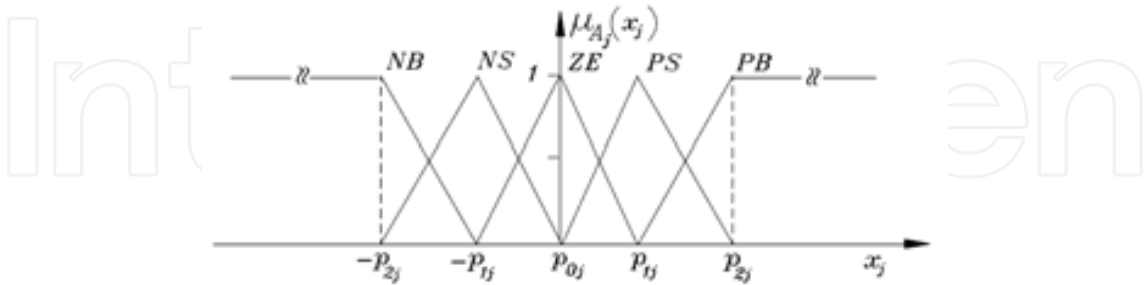


Fig. 9. Input membership functions

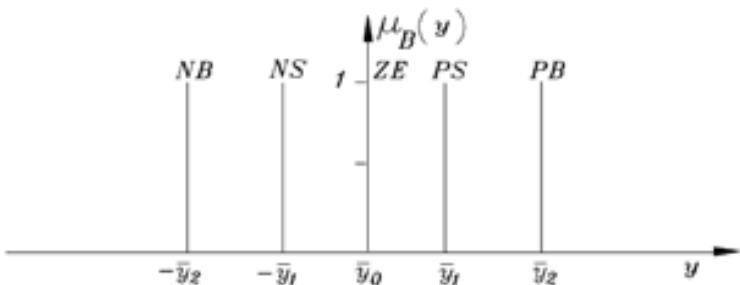


Fig. 10. Output membership functions

The fuzzy system considered here has following specifications: Singleton fuzzifier, triangular membership functions for each inputs, singleton membership functions for the output, rule base defined by (51), (see Table. 2), product inference and center average defuzzifier.

$x_1 \backslash x_2$	NB	NS	ZE	PS	PB
NB	NB	NB	NS	ZE	ZE
NS	NB	NB	NS	ZE	ZE
ZE	NS	NS	ZE	PS	PS
PS	ZE	ZE	PS	PB	PB
PB	ZE	ZE	PS	PB	PB

Table 2. The fuzzy rule base for obtaining output y

Thus, one can compute the output y in terms of inputs as follows (Wang, 1997):

$$y(x) = \varphi(x_1, x_2) = \frac{\sum_{l_1} \sum_{l_2} \bar{y}^{l_1 l_2} \left( \bigcap_{j=1}^2 \mu_{A_j^{l_j}}(x_j) \right)}{\sum_{l_1} \sum_{l_2} \left( \bigcap_{j=1}^2 \mu_{A_j^{l_j}}(x_j) \right)}$$

(52)



Special properties of this input-output mapping  $y(x)$  for  $x_1, x_2$  are given in (Santibanez et al., 2005).

**Lemma 2.3.** For the system with dynamical equation (30), if one chooses the following control law,

$$\tau = \varphi(\tilde{q}, \dot{\tilde{q}}) + G(q) \quad (53)$$

where  $\tilde{q}$  is defined as (38) and  $\dot{\tilde{q}} = \dot{q}_d - \dot{q}$  is velocity error vector, then the closed-loop system shown in Fig. 11 becomes stable.

*Proof:* the stability analysis is based on the study performed in (Calcev 1998) and is fully discussed in (Santibanez et al., 2005), so it is omitted here. Note that for constant set-point we have  $\dot{q}_d = 0$ , hence  $\dot{\tilde{q}} = -\dot{q}$ .

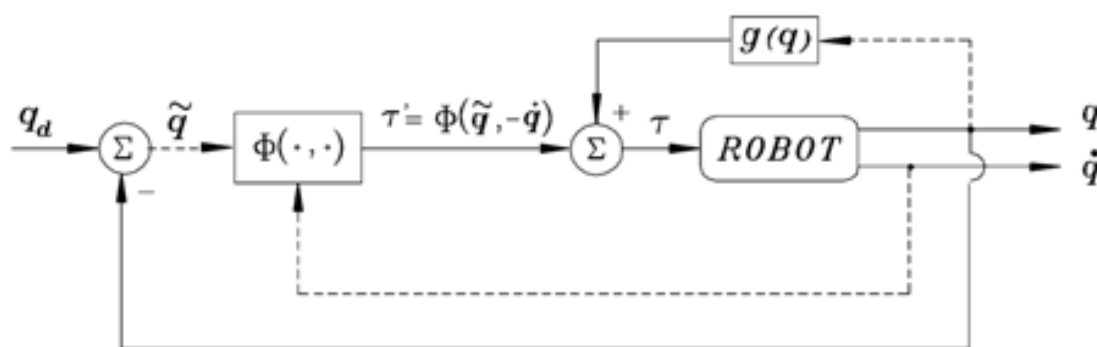


Fig. 11. Closed-loop system in the case of fuzzy controller (Santibanez et al., 2005)

## 2.2.4 Incorporating SMC and SFC

Each of the two controllers explained in last two subsections drives the robot joint angles to desired set-point in finite time and according to the Lemma 2.2 and 2.3 the closed-loop system is stable in both cases. In this section, for utilizing advantages of both sliding mode control and sectorial fuzzy control, and also minimizing the drawbacks of both of them, the following control law is proposed:

$$\tau = \begin{cases} \hat{\tau} - K \operatorname{sgn}(s) & \text{when } |q_e| \geq \alpha \\ y(q_e, \dot{q}_e) + G(q) & \text{when } |q_e| < \alpha \end{cases} \quad (54)$$

where  $\alpha$  is strictly positive small parameter which can be determined adaptively or set to a constant value. So, while the magnitude of error is greater than or equal to  $\alpha$ , SMC drives the system states, errors in our case, toward sliding surface and as soon as the magnitude of error becomes less than  $\alpha$ , then the SFC which is designed independent of initial conditions, controls the system. Since the SMC shows faster transient response, the response of the system controlled by (54) is faster than the case of SFC. Additionally, in spite of the torque boundedness, since the SFC controls the system in the steady state, the proposed controller (54) has less set-point tracking error. Also, since near the sliding surface the proposed controller switch from SMC to SFC, therefore, the chattering is avoided here.

**Simulation example 2.2.** In order to show the effectiveness of the proposed control law, it is applied to a two-link direct drive robot arm with the following parameters (Santibanez et al., 2005):

$$\begin{aligned}
 M(q) &= \begin{bmatrix} 2.351 + 0.168\cos(q_2) & 0.102 + 0.084\cos(q_2) \\ 0.102 + 0.084\cos(q_2) & 0.102 \end{bmatrix} \\
 \hat{C}(q, \dot{q}) &= \begin{bmatrix} -0.084\sin(q_2)\dot{q}_2 & -0.084\sin(q_2)(\dot{q}_1 + \dot{q}_2) \\ 0.084\sin(q_2)\dot{q}_1 & 0 \end{bmatrix} \\
 G(q) &= 9.81 \begin{bmatrix} 3.921\sin(q_1) + 0.186\sin(q_1 + q_2) \\ 0.186\sin(q_1 + q_2) \end{bmatrix} \\
 F(\dot{q}) &= \begin{bmatrix} 2.288\dot{q}_1 + 8.049\operatorname{sgn}(\dot{q}_1) + [1 - |\operatorname{sgn}(\dot{q}_1)|]\operatorname{sat}(\tau_1; 9.7) \\ 0.186\dot{q}_2 + 1.734\operatorname{sgn}(\dot{q}_2) + [1 - |\operatorname{sgn}(\dot{q}_2)|]\operatorname{sat}(\tau_2; 1.87) \end{bmatrix} \\
 C &= \hat{C} + \Delta C
 \end{aligned} \tag{55}$$

According to the actuators manufacturer, the direct drive motors are able to supply torques within the following bounds:

$$\begin{aligned}
 |\tau_1| &\leq \tau_1^{\max} = 150[\text{Nm}] \\
 |\tau_2| &\leq \tau_2^{\max} = 15[\text{Nm}]
 \end{aligned} \tag{56}$$

The desired set-point is,

$$q_d = [\pi \quad -\pi]^T \tag{57}$$

which is applied as a step function at time zero. The SMC design parameters are as below:

$$\lambda = \begin{bmatrix} 10 & 0 \\ 0 & 10 \end{bmatrix}, \Gamma = \begin{bmatrix} 140 \\ 8 \end{bmatrix} \text{ and } \phi = 5 \tag{58}$$

For SFC case, according to Fig. 9 and Fig. 11,  $p_{x_j} = \{-p_{2j}, -p_{1j}, p_{0j}, p_{1j}, p_{2j}\}$  is fuzzy partition of the input universe of discourse and  $p_y = \{-\bar{y}_2, -\bar{y}_1, \bar{y}_0, \bar{y}_1, \bar{y}_2\}$  is for output universe of discourse. Now, SFC design parameters are given by following equations (Santibanez et al., 2005):

$$\begin{aligned}
 p_{\bar{q}_1} &= \{-180, -4, 0, 4, 180\} \\
 p_{\bar{q}_2} &= \{-180, -2, 0, 2, 180\} \\
 p_{\dot{q}_1} &= \{-360, -270, 0, 270, 360\} \\
 p_{\dot{q}_2} &= \{-360, -270, 0, 270, 360\} \\
 p_{y_1} &= \{-109, -90, 0, 90, 109\} \\
 p_{y_2} &= \{-13, -9, 0, 9, 13\}
 \end{aligned} \tag{59}$$

For our proposed controller (54), the constant  $\alpha = 0.3$  is supposed. Additionally, to show the improvement achieved from applying the proposed method of this section (incorporating

SMC and SFC), the simulation results of applying this method are compared with the related results of the SMC case and SFC case, separately. The error vector and control law in the case of conventional SMC have been shown in Fig. 12 and Fig. 13, respectively.

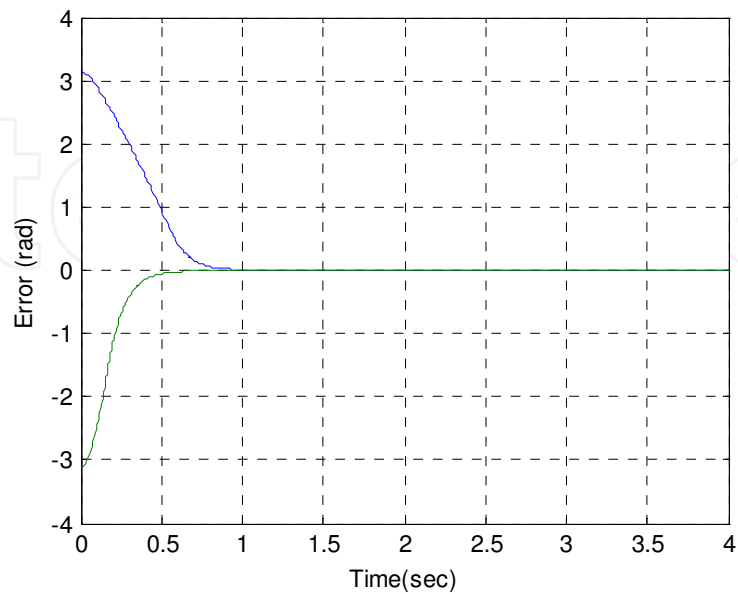


Fig. 12. Error vector in the case of SMC

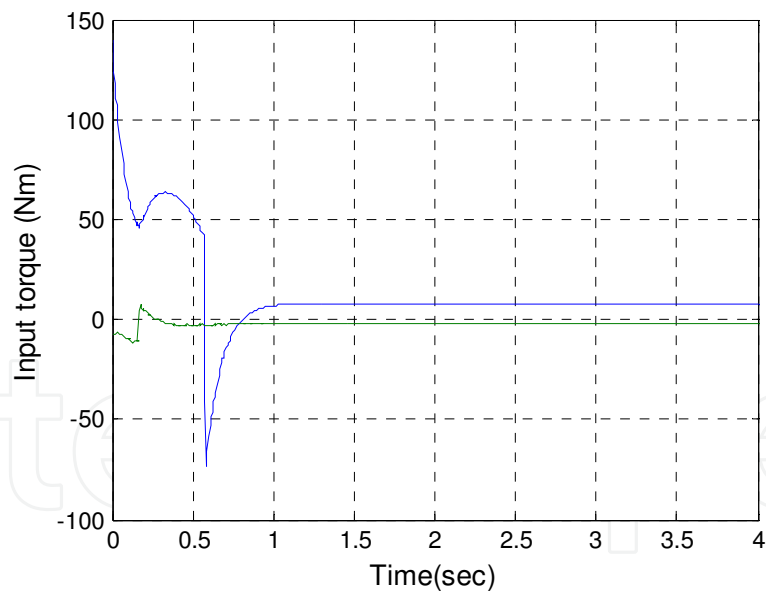


Fig. 13. The control torques in the case of SMC

The tracking error in this case is about 0.1(rad) and when one choose the thinner boundary layer to decrease this error, chattering will be occurred. The corresponding graphs for the case of applying SFC are also provided in Fig. 14, and Fig. 15.

In the case of control law proposed in the present section, Fig. 16 and Fig. 17 illustrate the error vector and control law, respectively. The tracking error is about 0.002 in this state of affairs.

As it can be seen from these results, the proposed incorporating SMC and SFC controller has faster response and less tracking error in comparison with SMC and also the error vector converges toward zero faster than SFC.

In order to show the robustness of the proposed method, the inertia and torque perturbations are considered as following. The elements of inertia matrix are supposed to increase fifty percent after 2 sec. It can be a weight that added to the mass of 2<sup>nd</sup> link. Also, disturbance torque is considered with the following equation.

$$\tau_d = [3 \sin 2\pi t \quad 3 \sin 2\pi t]^T$$

(60)

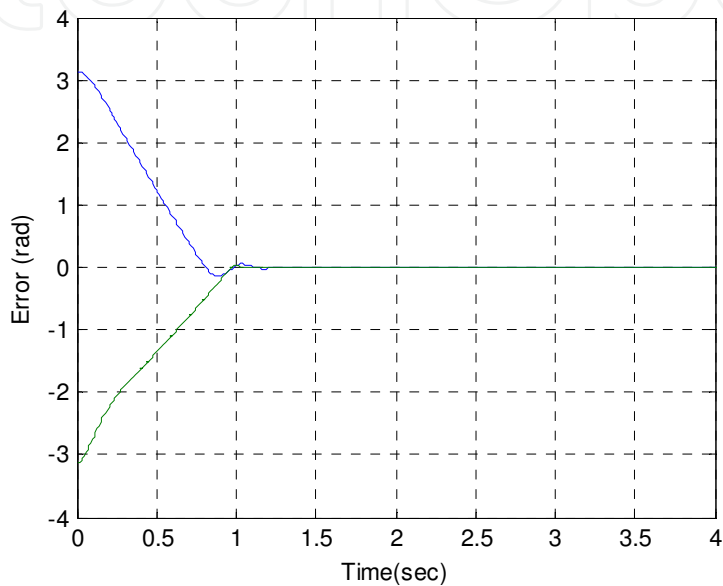


Fig. 14. Error vector in the case of SFC

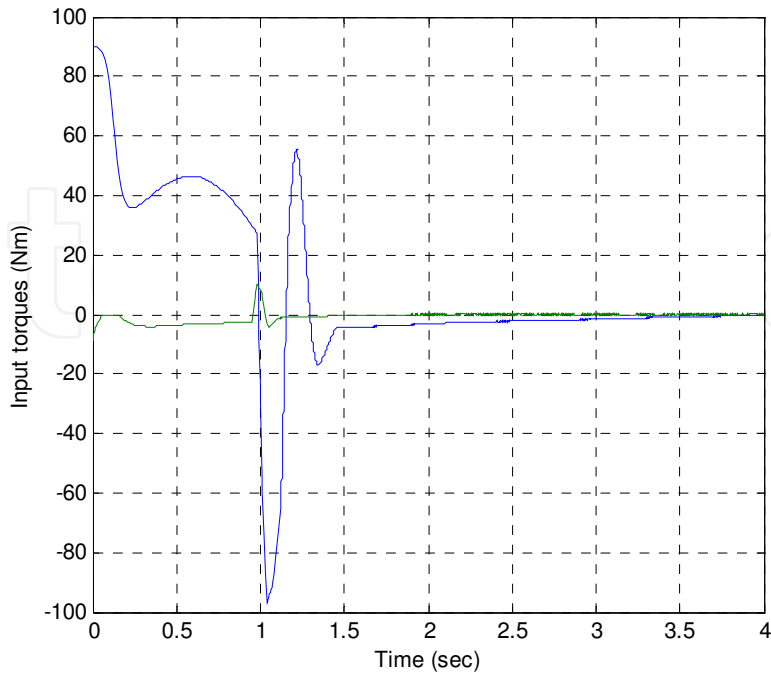


Fig. 15. The control torques in the case of SFC

In this case, the vector of joint errors is shown in Fig. 18. The errors are as good as previous case. Fig. 19 illustrates the control torques which are not change significantly, and because of existing perturbations, they alter trivially after 2 sec. these two recent results verify the robustness of the presented approach.

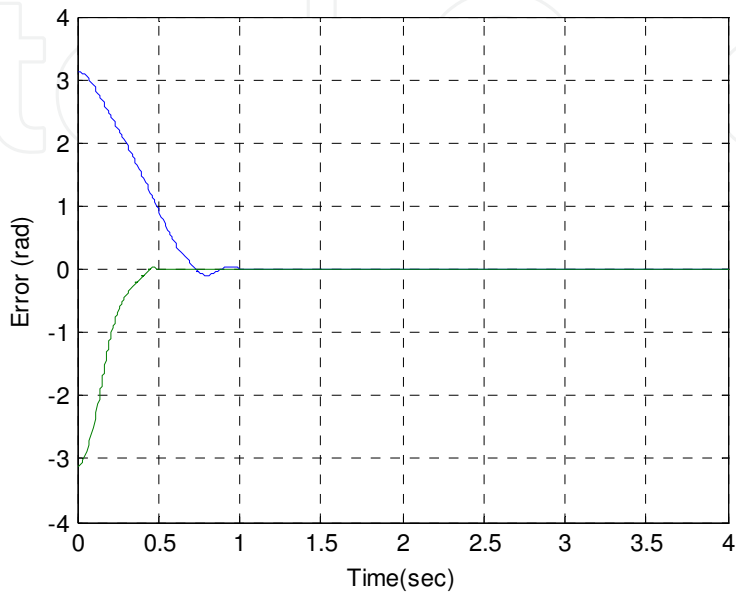


Fig. 16. Error vector in the case of incorporating SMC and SFC

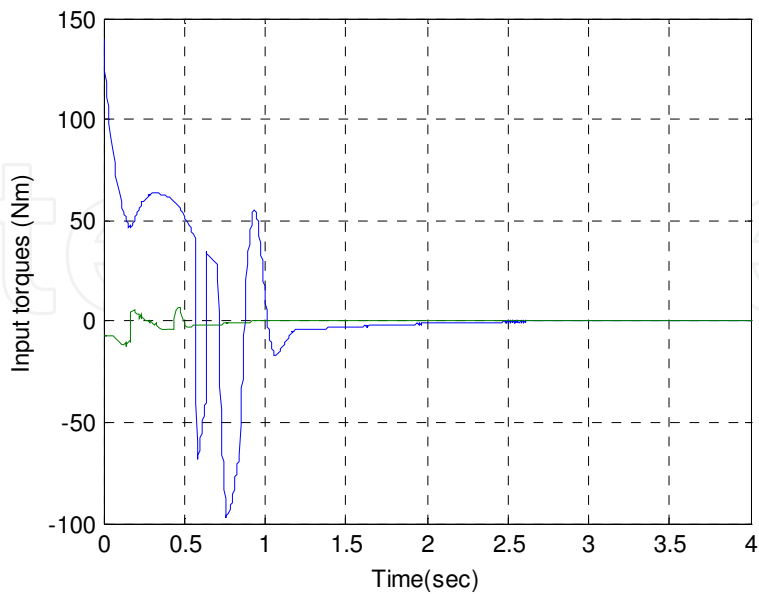


Fig. 17. The control torques in the case of incorporating SMC and SFC

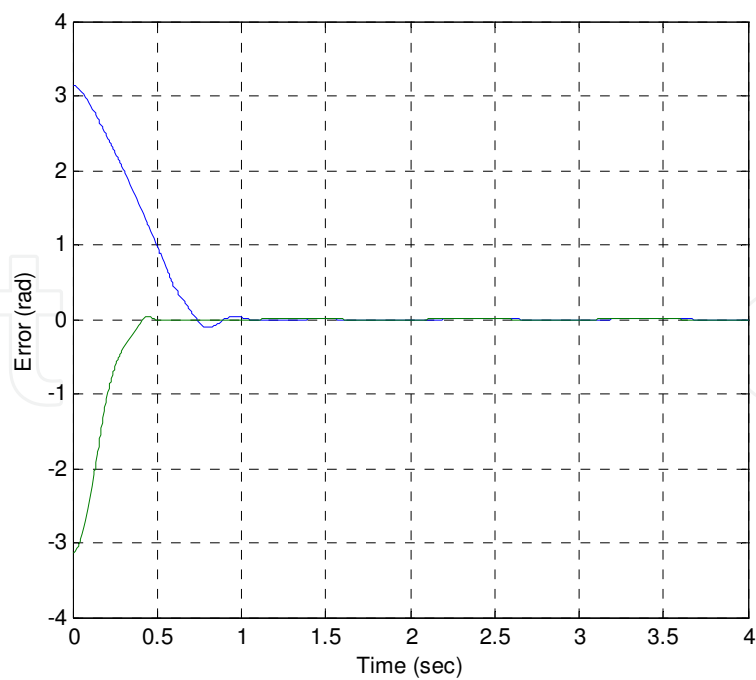


Fig. 18. Error vector in the case of torque and inertia perturbations

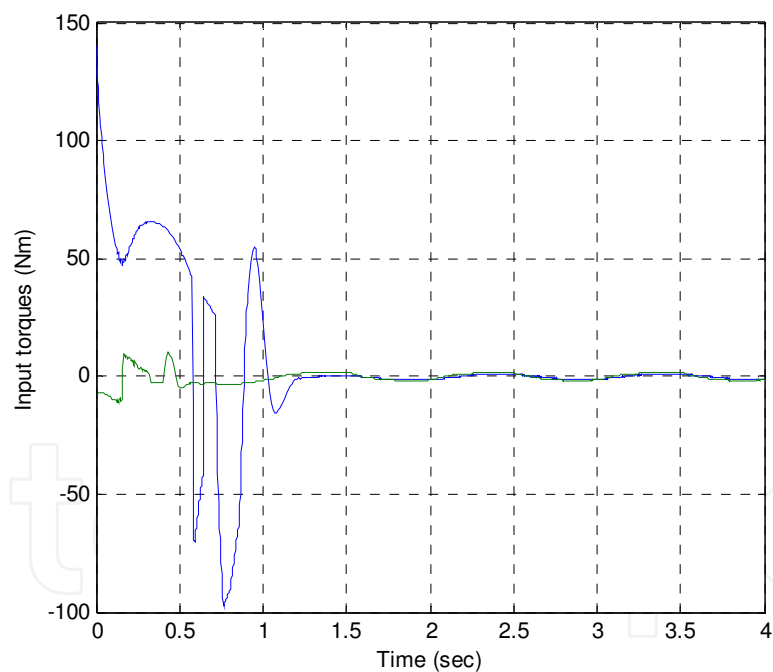


Fig. 19. The control torques in the case of torque and inertia perturbations

3. Sliding mode control using neural network approach

Sliding-Mode-PID control for robot manipulator was explored by (Ataei & Shafiei, 2008). In their study, although, the uncertainties are considered but controller design is extremely model-dependent. Also, control command starts with high gain and actuator dynamics is neglected. Moreover, stability analysis is not investigated after incorporating fuzzy tuning

system. A robust neural-fuzzy-network controller was designed in (Wai & Chen 2006) for the position control of an n-link robot manipulator including actuator dynamics. Although, their control scheme does not require compensating auxiliary control design, but the employed network is more complicated and uses excess number of neurons. In addition, the second derivative of position angle is required as a part of controller inputs. Capisani et al., (Capisani et al., 2009) presented an inverse dynamic-based second-order sliding mode controller to perform motion control of robot manipulators, but this method involves the higher order derivatives of the state variables.

In this section, the motion tracking control of multiple-link robot manipulators actuated by permanent magnet DC motors is addressed. Sliding-mode-PID tracking controller is designed such that all the states and signals of the closed loop system remain bounded in the presence of unknown parameters and uncertainties. Also, neural network universal approximation property is employed for compensating uncertainties. Furthermore, the proposed controller contains an outer PID-loop that enhances the approximation performance during the initial period of weight adaptations, and provides designing a simple NN with lower amount of layers and neurons. Adaptation laws are applied to adjust the NN weights on-line. In order to avoid high gain control, the gain factor of robustifying term is designed adaptively (Shafiei & Soltanpour, 2010).

### 3.1 Actuated robot dynamics

The mathematical equations describing electrical and mechanical dynamics of a permanent magnet DC motor are as follows (Spong & Vidyasagar, 1989):

$$V = Ri + L \frac{di}{dt} + K_b \frac{d\theta}{dt} \quad (61)$$

$$J_m \ddot{\theta} + B_m \dot{\theta} + \tau_m = \tau \quad (62)$$

$$\tau = K_m i \quad (63)$$

where  $V$  is the armature voltage of the motor,  $R$  and  $L$  are armature equivalent resistance and inductance, respectively,  $K_b$  is the back electromotive force constant,  $i$  is the armature current and  $\theta$  denotes the rotor position,  $J_m$  is the total moment of inertia,  $B_m$  is the damping coefficient,  $\tau_m$  and  $\tau$  represent the generated motor torque and the load torque, respectively, and  $K_m$  is the diagonal matrix of motor torque constant.

The dynamical equation of an n-link robot manipulator is in the standard form of (30) and is rewritten here.

$$M(q)\ddot{q} + C(q, \dot{q})\dot{q} + G(q) + F(\dot{q}) + \tau_d = \tau \quad (64)$$

Here,  $F(\dot{q}) \in R^n$  is the dynamic friction vector,  $\tau_d \in R^n$  denotes the vector of disturbance and un-modeled dynamics, and  $\tau$  is the torque vector.

With the purpose of increasing motion speed of the manipulators, motors are equipped with the high reduction gears as follows:

$$q = g_r \theta \quad (65)$$



and

$$\tau_m = g_r \tau \quad (66)$$

where  $g_r$  is the diagonal matrix of reduction ratio. In the following a practical constraint is considered.

**Constraint 3.1.** The maximum voltage that joint actuator can supply is  $V^{\max}$ . So, we have:

$$|V_i| \leq V_i^{\max}, \quad i = 1, \dots, n$$

It should be noted that, the applicable control input for driving robot arm is the armature voltage of the motors, here. So, by using equations (61)-(66) and neglecting the inductance  $L$ , because of its tiny amount, the following equation is achieved.

$$V = RK_m^{-1} \{ [J_m g_r^{-1} + g_r M] \ddot{q} + (B_m g_r^{-1} + g_r C + K_m R^{-1} K_b g_r^{-1}) \dot{q} + g_r G + g_r F(\dot{q}) + g_r \tau_d \} \quad (67)$$

The previous equation can be expressed in a compact form as:

$$U = D \ddot{q} + H + d \quad (68)$$

with  $U = V$  is the control command and the other parameters are

$$D = RK_m^{-1} (J_m g_r^{-1} + g_r M) \quad (69)$$

$$H = V_m + RK_m^{-1} [(B_m g_r^{-1} + K_m R^{-1} K_b g_r^{-1}) \dot{q} + g_r G(q)] \quad (70)$$

$$V_m = RK_m^{-1} g_r C(q, \dot{q}) \quad (71)$$

$$d = RK_m^{-1} g_r (F(\dot{q}) + \tau_d) \quad (72)$$

**Remark 3.1.** By noting that the parameters,  $R$ ,  $K_m$ ,  $J_m$  and  $g_r$  are positive definite diagonal matrices, the matrix  $D$  is symmetric and positive definite.

**Remark 3.2.** From relations (69) and (71), and property 2.2, the matrix  $(\dot{D} - 2V_m)$  is skew-symmetric too.

### 3.2 SMC- PID design and NN description

The tracking error could be defined as before as:

$$e = q_d - q \quad (73)$$

A key step in designing sliding mode controller is to introduce a proper sliding surface so that tracking errors and output deviations can be reduced to a satisfactory level (Eker, 2006). Accordingly, the sliding surface is considered as (74), containing the integral part in addition to the derivative term.

$$s = \dot{e} + \lambda_1 e + \lambda_2 \int_0^t e dt \quad (74)$$

where  $\lambda_i$  is diagonal positive definite matrix. Hence,  $s=0$  is a stable sliding surface and  $e \rightarrow 0$  as  $t \rightarrow \infty$ . Only defining the sliding surface as (74) is not adequate to claim that SMC-PID is designed, but the control effort must contain the independent PID part. For this purpose, the robot dynamic equations can be rewritten based on the sliding surface (in term of filtered error) as follows:

$$D\dot{s} = -V_m s + f - U \quad (75)$$

where

$$f(x) = D(\ddot{q}_d + \lambda_1 \dot{e} + \lambda_2 e) + V_m s + H + d \quad (76)$$

where  $D$ ,  $V_m$  and  $d$  are given by (69), (71) and (72) respectively, and

$$x = [\ddot{q}_d^T \quad s^T \quad \dot{q}^T]^T \quad (77)$$

Note that the input vector of  $s$  includes linear combination of  $e$  and  $\dot{e}$ , (i.e.  $\dot{e} + \lambda_1 e$ ) which they comprise  $q_d$ ,  $q$  and  $\dot{q}_d$ ,  $\dot{q}$ , too, respectively. The input dimension of the two-layer NN designed here is less than that of given by (Lewis et al., 1996), and thus the proposed method is more desirable from an implementation point of view. Sliding mode control strategy consists of designing a two-part controller.

$$U_{SMC} = U_{eq} + U_s \quad (78)$$

with  $U_{eq}$  is equivalent control part which is applied to cancel the uncertain nonlinear function  $f$ , and  $U_s$  specifies robust control term. Considering unknown parameter, uncertainties and disturbances indicates that the function  $f$  is not accessible. Briefly speaking, neural networks incorporate to reconstruct the  $U_{eq}$  part by approximating the function  $f$ , here. According to universal approximation property of neural networks (Lewis et al., 1998), there is a two-layer NN with sufficient number of neurons, and sigmoid or RBF activation function for hidden layer and linear activation function for output layer (see Fig. 20) such that:

$$f(x) = W^T \sigma(V^T x) + \varepsilon \quad (79)$$

where  $x \in R^{N_2}$  is the input vector computed by (77),  $V \in R^{N_2 \times N_2}$  and  $W \in R^{N_2 \times N_2}$  represents the NN weights for hidden and output layers, respectively,  $\sigma(\cdot)$  denotes activation function of the hidden layer and  $\varepsilon$  is NN approximation error. Choosing activation function is arbitrary provided that the function satisfies an approximation property and it and its derivative are bounded (Lewis et al., 1998), consequently the sigmoid activation function is considered, here.

$$\sigma(z) = \frac{1}{1 + e^{-z}} \quad (80)$$

Succeeding section explains complete controller design and investigates stability content.

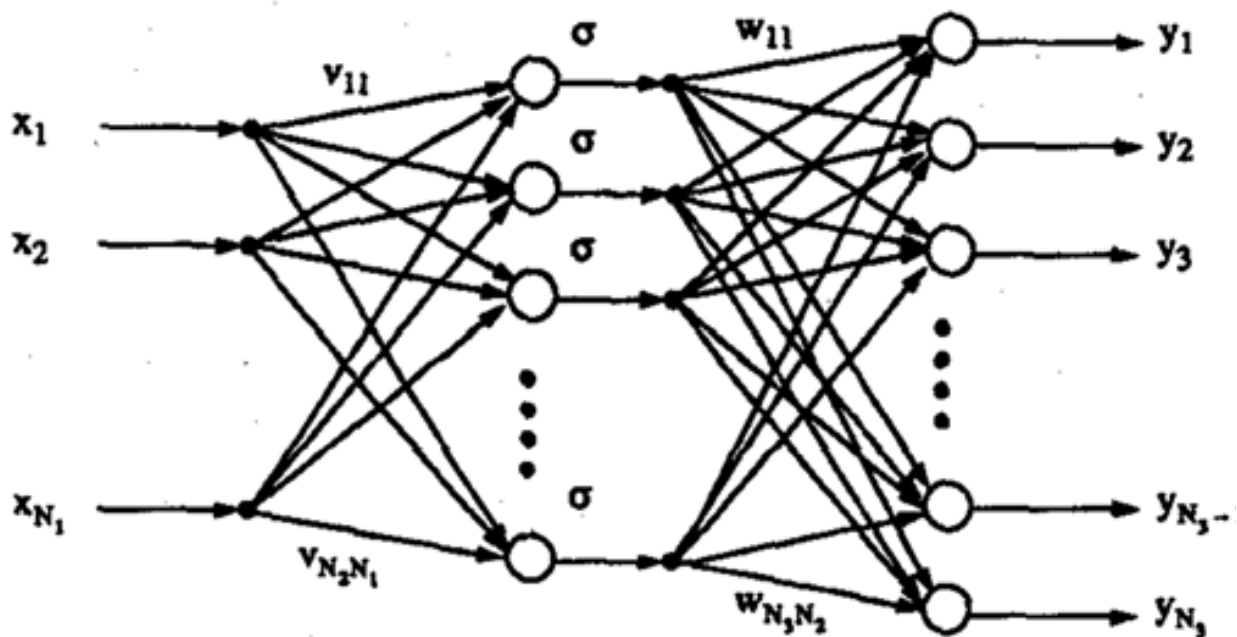


Fig. 20. Two-layer NN structure

### 3.3 Sliding mode control using adaptive neural network

Note that the utilized weights in (79) are optimum and  $f(x)$  is approximated ideally, over there. Estimation of  $f$  is accomplished by the estimated weights  $\hat{W}$  and  $\hat{V}$ , respectively. So, the NN controller is designed as:

$$\hat{f}(x) = \hat{W}^T \sigma(\hat{V}^T x) \quad (81)$$

here  $\hat{f}(x)$  is estimation of  $f(x)$  and  $\hat{W}$  and  $\hat{V}$  are updated adaptively. The estimation errors are defined as follows:

$$\tilde{V} = V - \hat{V}, \quad \tilde{W} = W - \hat{W} \quad (82)$$

also, the hidden layer output error for a given input  $x$  is

$$\tilde{\sigma} = \sigma(V^T x) - \sigma(\hat{V}^T x) = \sigma - \hat{\sigma} \quad (83)$$

Consider the  $\sigma(V^T x)$  as its Taylor series expansion as

$$\sigma(V^T x) = \sigma(\hat{V}^T x) + \sigma'(\hat{V}^T x) \tilde{V}^T x + O_h(\tilde{V}^T x) \quad (84)$$

where  $O_h(\cdot)$  denotes higher order terms in Taylor series and

$$\sigma'(z) \equiv \left. \frac{d\sigma(z)}{dz} \right|_{z=\hat{z}} \quad (85)$$

From (83) and (84), we have:

$$\tilde{\sigma} = \sigma'(\hat{V}^T x) \tilde{V}^T x + O_h(\tilde{V}^T x) = \hat{\sigma}' \tilde{V}^T x + O_h \quad (86)$$

Now, one can obtain overall error between optimum function  $f$  and its estimation  $\hat{f}$  as:

$$\begin{aligned} f - \hat{f} &= W^T \sigma(V^T x) + \varepsilon - \hat{W}^T \sigma(\hat{V}^T x) = \tilde{W}^T \sigma(V^T x) + \hat{W}^T \tilde{\sigma}(\hat{V}^T x) + \varepsilon \\ &= \tilde{W}^T [\sigma(\hat{V}^T x) + \sigma'(\hat{V}^T x) \tilde{V}^T x + O_h] + \hat{W}^T [\sigma'(\hat{V}^T x) \tilde{V}^T x + O_h] + \varepsilon \\ &= \tilde{W}^T \sigma(\hat{V}^T x) - \tilde{W}^T \sigma'(\hat{V}^T x) \tilde{V}^T x + \hat{W}^T \hat{\sigma}' \tilde{V}^T x + \tilde{W}^T \hat{\sigma}' V^T x + W^T O_h + \varepsilon \\ &= \tilde{W}^T \sigma(\hat{V}^T x) - \tilde{W}^T \sigma'(\hat{V}^T x) \tilde{V}^T x + \hat{W}^T \hat{\sigma}' \tilde{V}^T x + \varepsilon_N \end{aligned} \quad (87)$$

where

$$\varepsilon_N = \tilde{W}^T \hat{\sigma}' V^T x + W^T O_h + \varepsilon \quad (88)$$

is the uncertain term and is supposed to be bounded by  $K$  as demonstrated in (89).

$$\|\varepsilon_N\| \leq \|\tilde{W}^T \hat{\sigma}' V^T x\| + \|W^T O_h\| + \|\varepsilon\| < K \quad (89)$$

Design of the control system is provided in the following theorem and is illustrated in Fig. 21 schematically.

**Theorem 3.1.** Robot manipulator including actuator dynamics represented by equation (68) is considered, and the sliding surface is defined by (74). If the control input  $U$  is designed as (90) together with adaptation laws of NN controller as (91)-(93), then the asymptotic stability of the dynamical system is guaranteed.

$$U = K_v s + \hat{f} + \hat{K} \operatorname{sgn}(s) \quad (90)$$

$$\dot{\hat{W}} = \alpha \sigma(\hat{V}^T x) s^T - \alpha \hat{\sigma}' \hat{V}^T x s^T \quad (91)$$

$$\dot{\hat{V}} = \beta x s^T \hat{W}^T \hat{\sigma}' \quad (92)$$

$$\dot{\hat{K}} = \gamma s^T \operatorname{sgn}(s) \quad (93)$$

where  $K_v$  is a positive definite diagonal matrix,  $\hat{K}$  is the estimated value of  $K$ . Also,  $\alpha$ ,  $\beta$  and  $\gamma$  are positive constants and  $\operatorname{sgn}(\cdot)$  denotes sign function.

*Proof:* consider the following Lyapunov function candidate

$$V_L = \frac{1}{2} s^T D s + \frac{1}{2\alpha} \operatorname{tr}(\tilde{W}^T \tilde{W}) + \frac{1}{2\beta} \operatorname{tr}(\tilde{V}^T \tilde{V}) + \frac{1}{2\gamma} \tilde{K}^T \tilde{K} \quad (94)$$

where  $\operatorname{tr}(\cdot)$  denotes the trace operator and  $\tilde{K} = K - \hat{K}$ . Differentiating of the relation (94) gives

$$\dot{V}_L = s^T D \dot{s} + \frac{1}{2} s^T \dot{D} s + \frac{1}{\alpha} \operatorname{tr}(\tilde{W}^T \dot{\tilde{W}}) + \frac{1}{\beta} \operatorname{tr}(\tilde{V}^T \dot{\tilde{V}}) + \frac{1}{\gamma} \tilde{K}^T \dot{\tilde{K}} \quad (95)$$

By substituting (90) in to the first part of (95) and by using (87) one can obtain

$$\begin{aligned} S^T D \dot{s} &= s^T [-V_m s + f - U] = s^T [-V_m s + f - K_v s - \hat{f} - \hat{K} \operatorname{sgn}(s)] \\ &= s^T [-V_m s - K_v s + \tilde{W}^T \hat{\sigma} - \tilde{W}^T \hat{\sigma}' \hat{V}^T x + \hat{W}^T \hat{\sigma}' \tilde{V}^T x + \varepsilon_N - \hat{K} \operatorname{sgn}(s)] \end{aligned} \quad (96)$$

Some useful relations for manipulating last tow equations are provided in the following.

$$\begin{cases} s^T \tilde{W}^T \hat{\sigma} = \operatorname{tr}(\tilde{W}^T \hat{\sigma} s^T) \\ s^T \tilde{W}^T \hat{\sigma}' \hat{V}^T x = \operatorname{tr}(\tilde{W}^T \hat{\sigma}' \hat{V}^T x s^T) \\ s^T \hat{W}^T \hat{\sigma}' \tilde{V}^T x = \operatorname{tr}(\tilde{V}^T x s^T \hat{W}^T \hat{\sigma}') \end{cases}$$

Replacing (96) in (95) and using above relations, produce

$$\begin{aligned} \dot{V}_L &= -s^T K_v s + \frac{1}{2} s^T (\dot{D} - 2V_m) s + \operatorname{tr} \left[ \tilde{W}^T \left( \frac{1}{\alpha} \dot{\tilde{W}} + \hat{\sigma} s^T - \hat{\sigma}' \hat{V}^T x s^T \right) \right] \\ &\quad + \operatorname{tr} \left[ \tilde{V}^T \left( \frac{1}{\beta} \dot{\tilde{V}} + x s^T \hat{W}^T \hat{\sigma}' \right) \right] + s^T \varepsilon_N - \hat{K} s^T \operatorname{sgn}(s) + \frac{1}{\gamma} \dot{\tilde{K}} \dot{K} \end{aligned} \quad (97)$$

Note that  $\dot{\tilde{W}} = -\dot{\hat{W}}$ ,  $\dot{\tilde{V}} = -\dot{\hat{V}}$ ,  $\dot{\tilde{K}} = -\dot{\hat{K}}$ , and Remark 3.2 yields  $s^T (\dot{D} - 2V_m) s = 0$ . Also, if adaptive laws (91) and (92) are taken in to account, then we have

$$\dot{V}_L = -s^T K_v s + s^T \varepsilon_N - \hat{K} s^T \operatorname{sgn}(s) - \frac{1}{\gamma} (K - \hat{K}) \dot{\hat{K}} = -s^T K_v s + s^T \varepsilon_N - K s^T \operatorname{sgn}(s) \quad (98)$$

substituting (93) in (98) and adopting (99), yields

$$\dot{V}_L \leq -K_{v_{\min}} \|s\|^2 + \|\varepsilon_N\| (\|s_1\| + \|s_2\| + \dots + \|s_m\|) - K \sum_{i=1}^m \|s_i\| \leq -K_{v_{\min}} \|s\|^2 \leq 0 \quad (99)$$

where  $K_{v_{\min}}$  is minimum singular value of  $K_v$ . Since  $\dot{V}_L \leq 0$ , the stability in the sense of Lyapunov is guaranteed which implies that the parameters  $s$ ,  $\tilde{W}$ ,  $\tilde{V}$  and  $\tilde{K}$  (and consequently  $\hat{W}$ ,  $\hat{V}$ ,  $\hat{K}$ ) are bounded. In addition,  $\lim_{t \rightarrow \infty} \int_0^t -\dot{V}_L d\tau < \infty$  and  $-\dot{V}_L$  is bounded, hence Barbalat's Lemma (Khalil, 2001) indicates that  $\lim_{t \rightarrow \infty} (-\dot{V}_L) = 0$ . Note that  $(-\dot{V}_L) \geq K_{v_{\min}} \|s\|^2 \geq 0$ , as a result  $s \rightarrow 0$  as  $t \rightarrow \infty$ . Therefore, the proposed control system is asymptotically stable.

**Remark 3.3.** The PID term in the above control effort, makes Lyapunov derivative more negative, so it makes the transient response faster and also ensures the performance efficiency during the initial period of weights adaptations.

**Remark 3.4.** In practical systems, however, it is impossible to achieve infinitely fast switching control, because of finite time delays for the control computation and limitation of physical actuators. For that reason, the sign function is replaced by saturation function here, and the stability matter is investigated analytically.

The saturation function is selected as

$$\text{sat}\left(\frac{s}{\varphi}\right) = \begin{cases} \frac{s}{\varphi} & \|s\| \leq \varphi \\ \text{sgn}\left(\frac{s}{\varphi}\right) & \|s\| \geq \varphi \end{cases} \quad (100)$$

where  $\varphi$  is a thin boundary layer such that  $0 < \varphi \leq 1$ . The adaptive law (93) must be replaced by  $\dot{\hat{K}} = \gamma s^T \text{sat}(s/\varphi)$ ; So, the equation (98) is changed to

$$\dot{V}_L = -s^T K_v s + s^T \varepsilon_N - K s^T \text{sat}(s/\varphi) \quad (101)$$

Now, there are two situations;

a. if  $\|s\| > \varphi$ , then

$$\dot{V}_L \leq -K_{v_{\min}} \|s\|^2 + \|\varepsilon_N\| (\|s_1\| + \|s_2\| + \dots + \|s_m\|) - K \sum_{i=1}^m \|s_i\| < 0 \quad (102)$$

b. if  $\|s\| \leq \varphi$ , then

$$\dot{V}_L \leq -K_{v_{\min}} \|s\|^2 + \|\varepsilon_N\| (\|s_1\| + \|s_2\| + \dots + \|s_m\|) - \frac{K}{\varphi} \sum_{i=1}^m \|s_i\| < 0 \quad (103)$$

Note that, since  $0 < \varphi < 1$ , therefore  $\frac{K}{\varphi} \geq K > \|\varepsilon_N\|$ . Both situations imply that  $\dot{V}_L < 0$ , and consequently, the control system remains stable after replacing saturation function.

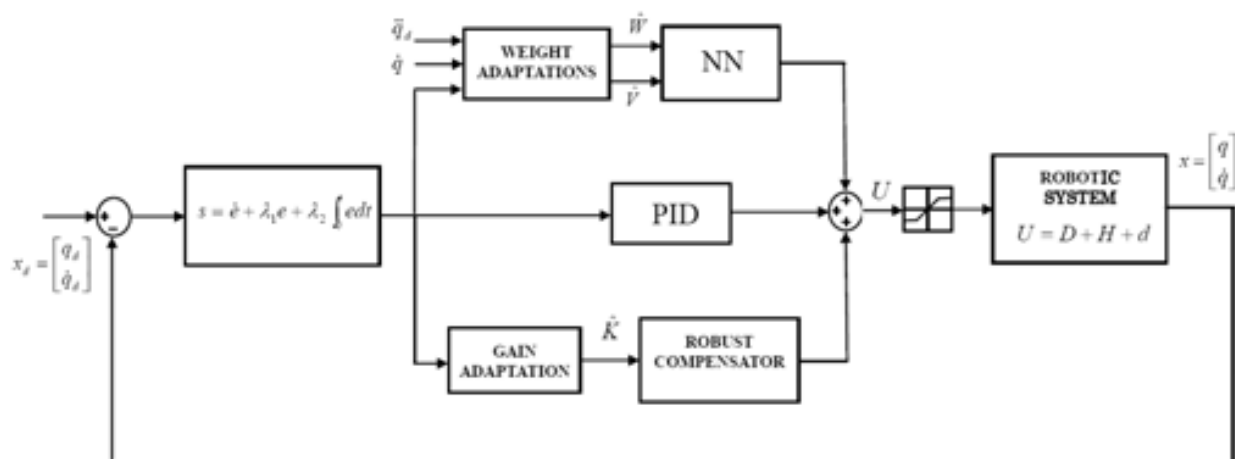


Fig. 21. Block diagram of the control system structure

**Remark 3.5.** The sliding gain  $\hat{K}$  is chosen dynamically and its dynamic depends on sliding surface. When the states go far from the sliding manifold, the absolute value of  $\hat{K}$  increases to force them back to sliding manifold, and when the states are close to the sliding manifold, the absolute value of  $\hat{K}$  decreases accordingly. This feature beside the replacing saturation function, act as what is heuristically designed by fuzzy system in (Ataei & Shafiei, 2008). Furthermore, the system stability is addressed here.

**Simulation example 3.1.** In order to show the effectiveness of the proposed control method, it is applied to a two-link elbow robot driven by permanent magnet DC motors with the following parameters:

$$\begin{aligned} M(q) &= \begin{bmatrix} m_1 l_{c1}^2 + m_2 (l_1^2 + l_{c2}^2 + 2 l_1 l_{c2} \cos q_2) & m_2 (l_{c2}^2 + l_1 l_{c2} \cos q_2) \\ m_2 (l_{c2}^2 + l_1 l_{c2} \cos q_2) & m_2 l_{c2}^2 \end{bmatrix} \\ C(q, \dot{q}) &= \begin{bmatrix} -m_2 l_1 l_{c2} \sin(q_2) \dot{q}_2 & -m_2 l_1 l_{c2} \sin(q_2) (\dot{q}_1 + \dot{q}_2) \\ m_2 l_1 l_{c2} \sin(q_2) \dot{q}_1 & 0 \end{bmatrix} \\ G(q) &= \begin{bmatrix} m_1 g l_{c1} \cos q_1 + m_2 g l_1 \cos q_1 + m_2 g l_{c2} \cos(q_1 + q_2) \\ m_2 g l_{c2} \cos(q_1 + q_2) \end{bmatrix} \end{aligned} \tag{104}$$

where  $q_i$  is the angle of joint  $i$ ,  $m_i$  is the mass of link  $i$ ,  $l_i$  is the total length of link  $i$ ,  $l_{ci}$  is center-of-gravity length of link  $i$ , and  $g = 9.8 \text{ m/s}^2$  is gravity acceleration. The detailed parameters of this robot manipulator and permanent magnet DC motor actuators are provided in Table 3 (Wai & Chen, 2006). According to the actuator manufacturer, the DC motors are able to accept input voltages within the following bounds:

$$V_1 \leq V_1^{\max} = 12 \text{ [volt]}, \quad V_2 \leq V_2^{\max} = 12 \text{ [volt]} \tag{105}$$

For example, one can use 12V DC servo motors for actuating joints. In practice, also, a servo control card is required which should include multi-channels of digital/analog (D/A) and encoder interface circuits.

Two-link elbow robot		Permanent-magnet DC motors	
$m_1 = 3.55 \text{ kg}$	$m_2 = 0.75 \text{ kg}$	$J_{m1} = 3.7 \times 10^{-5} \text{ kg.m}^2$	$J_{m2} = 1.47 \times 10^{-4} \text{ kg.m}^2$
$l_1 = 205 \text{ mm}$	$l_2 = 210 \text{ mm}$	$B_{m1} = 1.3 \times 10^{-5} \text{ N.m/s}$	$B_{m2} = 2 \times 10^{-5} \text{ N.m/s}$
$l_{c1} = 154.8 \text{ mm}$	$l_{c2} = 105 \text{ mm}$	$R_1 = 2.8 \text{ }\Omega$	$R_2 = 4.8 \text{ }\Omega$
$K_{m1} = 0.21 \text{ Nm/A}$	$K_{m2} = 0.23 \text{ Nm/A}$	$L_1 = 3 \text{ mH}$	$L_2 = 2.4 \text{ mH}$
$g_{r1} = 1/60$	$g_{r2} = 1/30$	$K_{b1} = 2.42 \times 10^{-4} \text{ s/rad.V}$	$K_{b2} = 2.18 \times 10^{-4} \text{ s/rad.V}$

Table 3. Parameters of two-link elbow robot and actuators

The external disturbances can be considered as external forces injected into the robotic system, and are supposed to have following expression.

$$\tau_d = [\sin 4t \quad \sin 4t]^T \tag{106}$$

Also, the friction term is considered here as (Wai & Chen, 2006):

$$F(\dot{q}) = [20\dot{q}_1 + 0.8 \operatorname{sgn}(\dot{q}_1) \quad 4\dot{q}_2 + 0.16 \operatorname{sgn}(\dot{q}_2)]^T \tag{107}$$

In order to show the effectiveness of proposed controller in tracking of desired trajectory, it is assumed to have the sinusoidal shape in this simulation.

$$q_d = [\sin t \quad \sin t]^T \tag{108}$$

The design parameters are given in Table 4. The gain matrices  $\lambda_1$  and  $\lambda_2$  are selected such that the roots of the characteristic polynomial  $\ddot{e} + \lambda_1 \dot{e} + \lambda_2 e = 0$  lie strictly in the open left half



of the complex plane when the system is in sliding mode ( $\dot{s}=0$ ). The neural network designed here has four neurons as hidden layer and two neurons as output layer, and its weights are totally initialized at zero.

*Remark 3.6.* For a two-layer NN designed here with the input vector given by (77), we have  $N_1 = 6$ ,  $N_2 = 4$  and  $N_3 = 2$ , for a two-link manipulator. Accordingly, the numbers of adaptive weights are 24 and 8 for input-to-hidden layer weights and output layer weights, respectively. So, only 32 weight parameters must be adaptively updated here while using the NN given in (Lewis et al., 1996), with  $N_1 = 10$ ,  $N_2 = 10$  and  $N_3 = 2$ , this number increases to 120. If the network size is chosen to large, the improvement of control performance is limited and the computation burden for the CPU is significantly increased.

The gain matrix  $K_v$  which acts as the gain of the PID term is determined large enough to improve transient response in the initial period of weight adaptations. On the other hand, choosing  $K_v$  to a large extent increases the overall controller gain and may exceed the permissible voltages of the actuators that are regarded in constraint 3.1. So, there is a trade off between fast response and practical limitations.

$\lambda_1 = \begin{bmatrix} 10 & 0 \\ 0 & 10 \end{bmatrix}$	$\lambda_2 = \begin{bmatrix} 24 & 0 \\ 0 & 24 \end{bmatrix}$	$g_r = \begin{bmatrix} 1/60 & 0 \\ 0 & 1/30 \end{bmatrix}$	$K_v = \begin{bmatrix} 5 & 0 \\ 0 & 5 \end{bmatrix}$
$\alpha = 5$	$\beta = 5$	$\gamma = 2$	$\varphi = 0.05$

Table 4. Design parameters

The mass variation of second link, the external disturbance and the friction are the major factors that affect the control performance of the robotic system. In the reminder of this section, two simulation cases are carried out to show the improvement due to the NNSM\_PID control method proposed in this section. In both cases, the simulation results of applying presented method are compared with the related results of the fuzzy sliding mode\_PID (FSM\_PID) control method proposed in (Ataei & Shafiei, 2008). In the first case, the disturbance (106) and mass variation are injected and in the second case, the friction term is exerted too. The mass variation condition is that 1 kg weight is added to the mass of 2<sup>nd</sup> link (i.e.  $m_2 = 1.75$  kg). For the FSM\_PID case, the control law is as following (Ataei & Shafiei, 2008):

$$U_f = K_{vf}s + \hat{f}_f + K_f \operatorname{sgn}(s)$$

(109)

$$K_{vf} = N_{vf} K_{fuzzy}$$

(110)

$$K_f = N_f K_{fuzzy}$$

(111)

where,  $U_f$  is the control input,  $K_{fuzzy}$  is of fuzzy system output and  $N_{vf}$  and  $N_f$  are the scaling gain of the fuzzy system output. Here, it is assumed that only manipulator parameters could be estimated and actuator parameters are still unknown. So,  $\hat{f}_f$  is chosen as (Ataei & Shafiei, 2008):

$$\hat{f}_f = \hat{M}(\ddot{q}_d + \lambda_1 \dot{e} + \lambda_2 e) + \hat{C}(\dot{q}_d + \lambda_1 e + \lambda_2 \int_0^t e dt) + \hat{G}$$

(112)

where  $\hat{M}$ ,  $\hat{C}$  and  $\hat{G}$  are achieved from nominal value of manipulator parameters. However, all of the manipulator parameters are considered with 10% uncertainty. The design parameters of the FSM\_PID controller are

$$N_{vf} = \begin{bmatrix} 3.2 & 0 \\ 0 & 3.5 \end{bmatrix}, N_f = \begin{bmatrix} 0.8 & 0 \\ 0 & 0.7 \end{bmatrix} \quad (113)$$

**Simulation 1—** In this case, the friction term is neglected, mass variation occurs at 3 sec and external disturbance is injected at 6 sec. The desired trajectory is depicted in Fig. 22. The vectors of tracking errors of FSM\_PID and NNSM\_PID are shown in Fig. 23 (a) and (b), respectively. Both diagrams of Fig. 23 are plotted in the same scaled axes to achieve fairly comparison. The FSM\_PID controller does not meet the tracking purpose in the unknown actuator parameters and mass variation conditions. On the contrary, the method proposed in this section provides swift and precise tracking responses. Fig. 24 displays the control efforts (i.e. input armature voltages of motors). The FSM\_PID associated control commands are jagged to some extent, while, the NNSM\_PID case produces smooth control commands with slowly variation and lower voltage amplitude. Lower voltage commands are more protected toward actuator saturations. The NN outputs are shown in Fig. 25 and it indicates that the designed neural network can approximate nonlinear terms with unknown parameters, smoothly and boundedly.

**Simulation 2—** With the purpose of showing robustness of our designed controller against uncertainties and un-modeled dynamics, the friction term (107) is added here. The vectors of tracking errors of FSM\_PID and NNSM\_PID are shown in Fig. 26 (a) and (b), respectively. However, the response of the FSM\_PID case is further undesirable in this condition, on the other hand, the NNSM\_PID control remains robust and its response is satisfactory, as well as previous simulation case. Control efforts of this case are demonstrated in Fig. 27. Because of exerting friction term, the input voltage commands are higher than previous case but the NNSM\_PID control commands are still smooth and vary slowly. The NN output is shown in Fig. 28. Finally, as can be seen from Fig. 29, matrix norm of the adaptive weights,  $\|\hat{W}\|$  and  $\|\hat{V}\|$ , have bounded value, less than 3, that it verifies what was claimed in the Theorem 3.1 about boundedness of these signals.

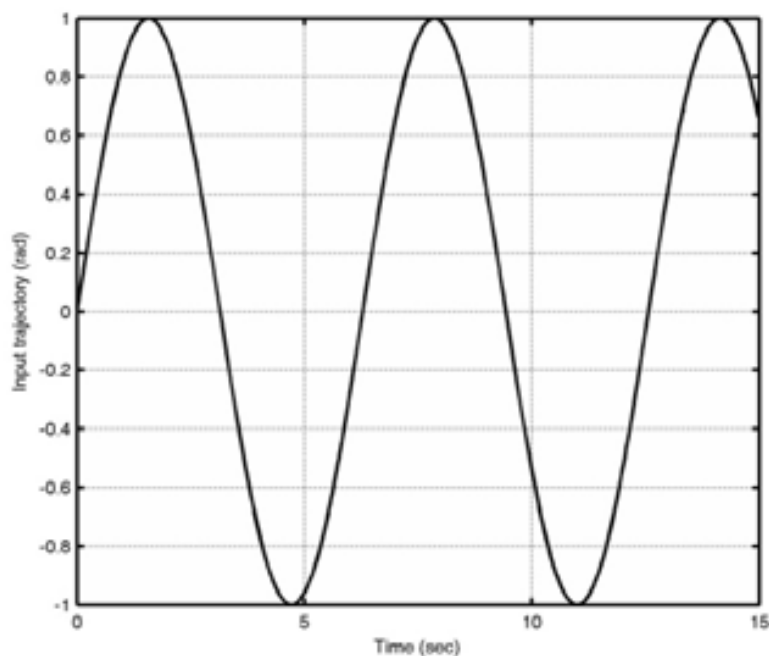


Fig. 22. Desired input trajectory  $q_d$

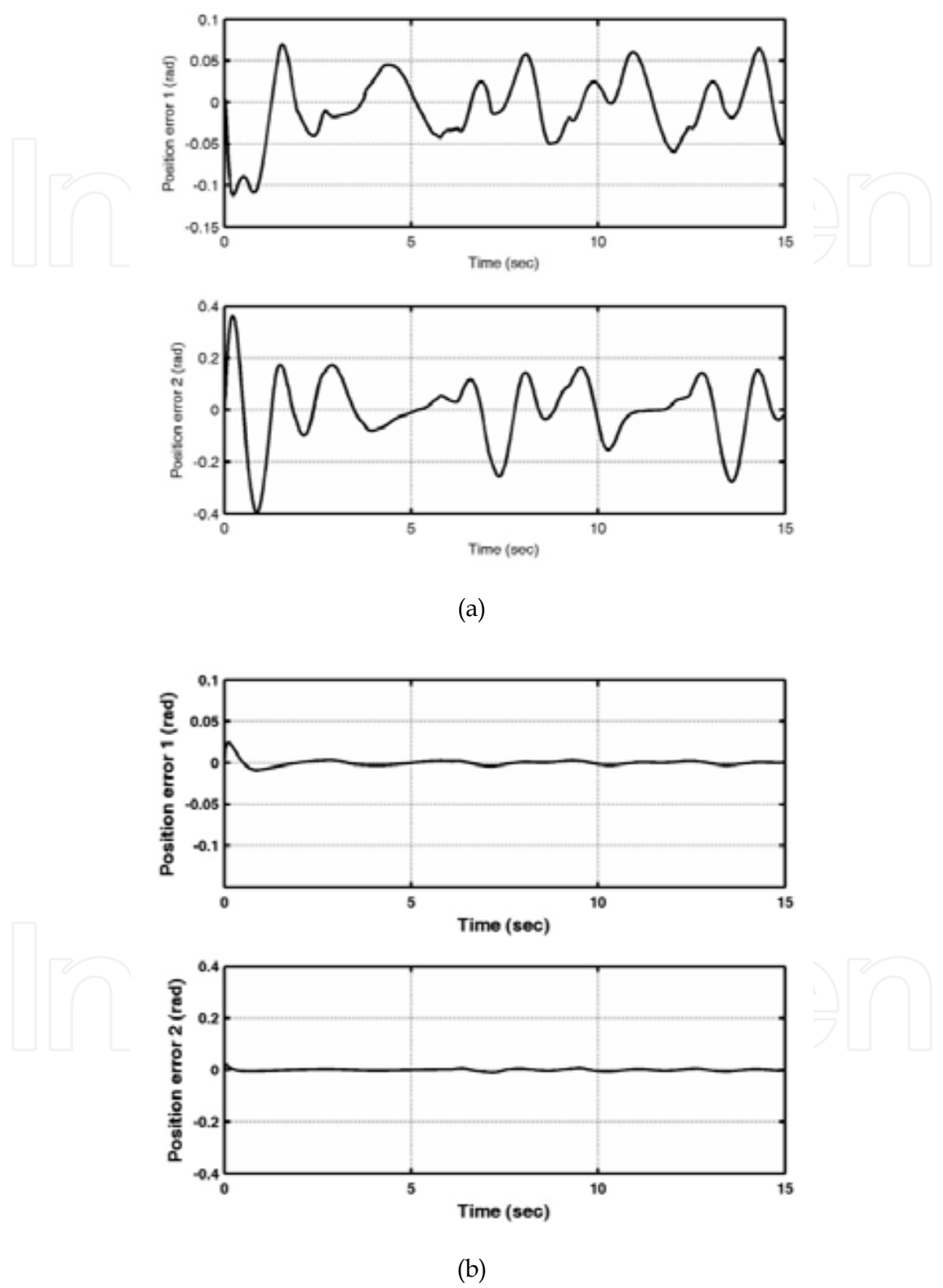
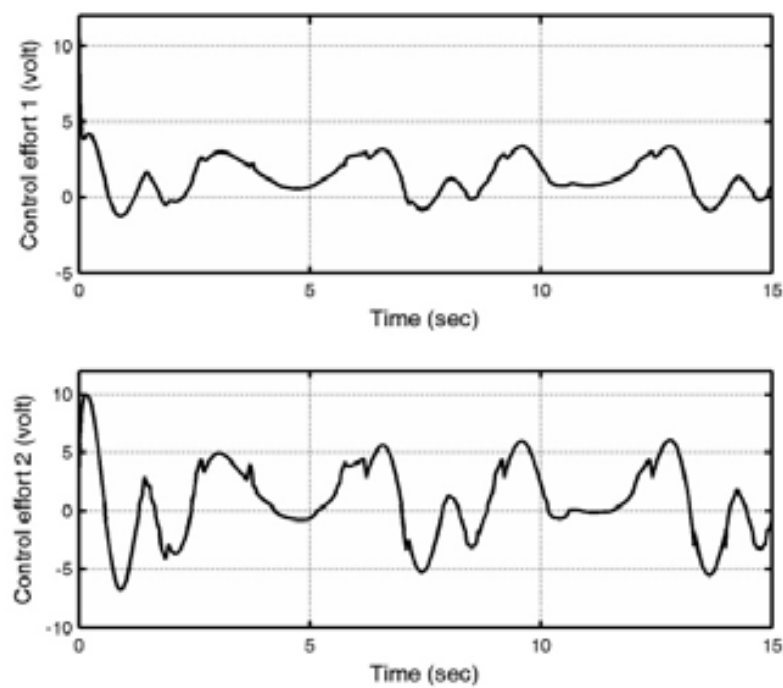
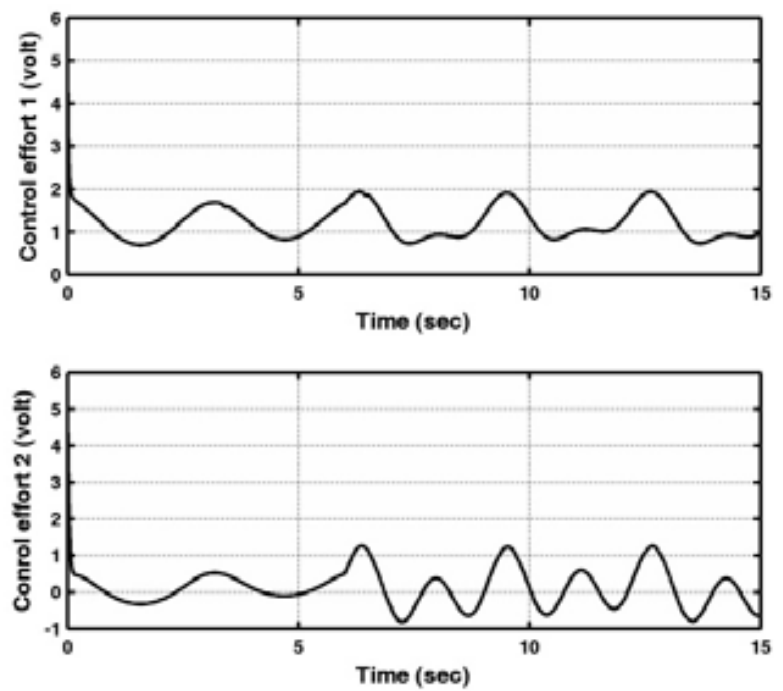


Fig. 23. (sim1) Tracking error of joints, (a) FSM\_PID (b) NNSM\_PID



(a)



(b)

Fig. 24. (sim1) Control commands (a) FSM\_PID (b) NNSM\_PID

IntechOpen

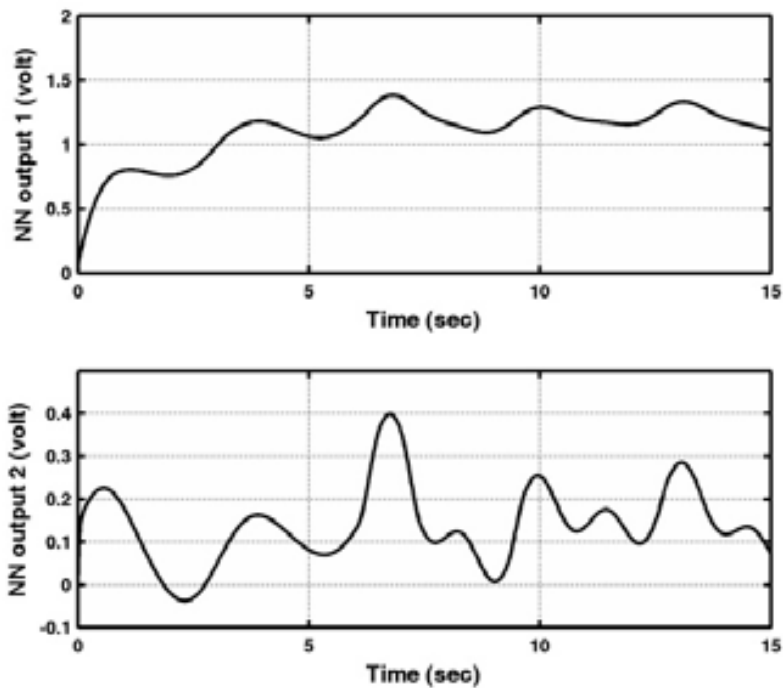
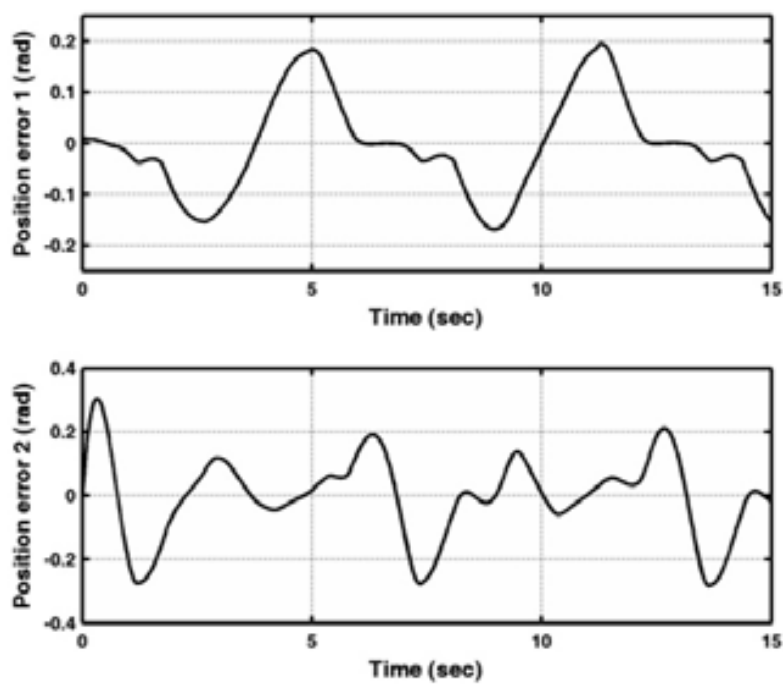
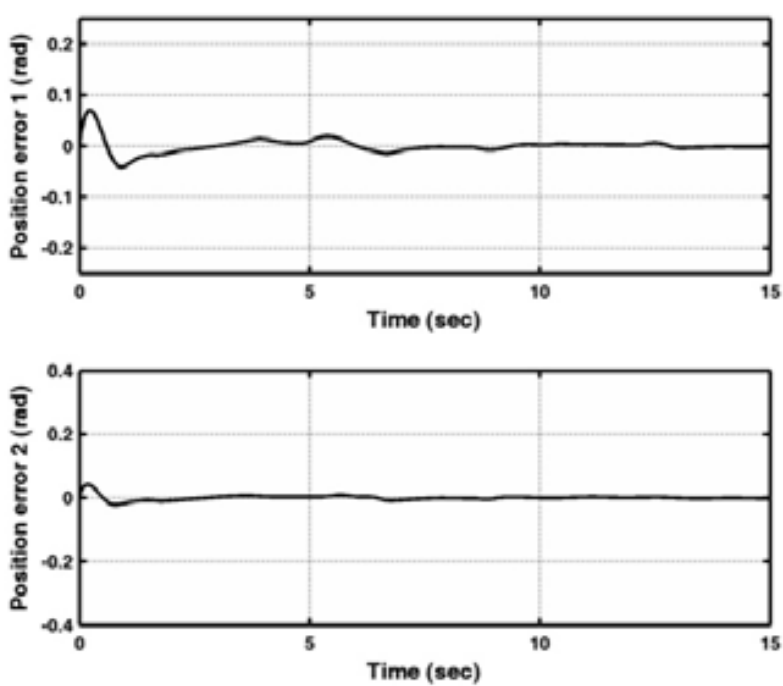


Fig. 25. (sim1) NN control effort

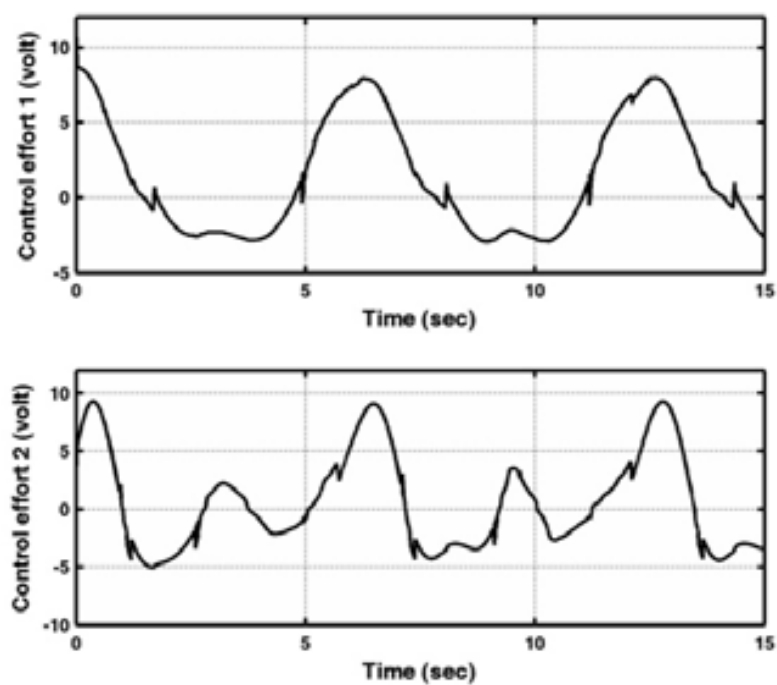


(a)

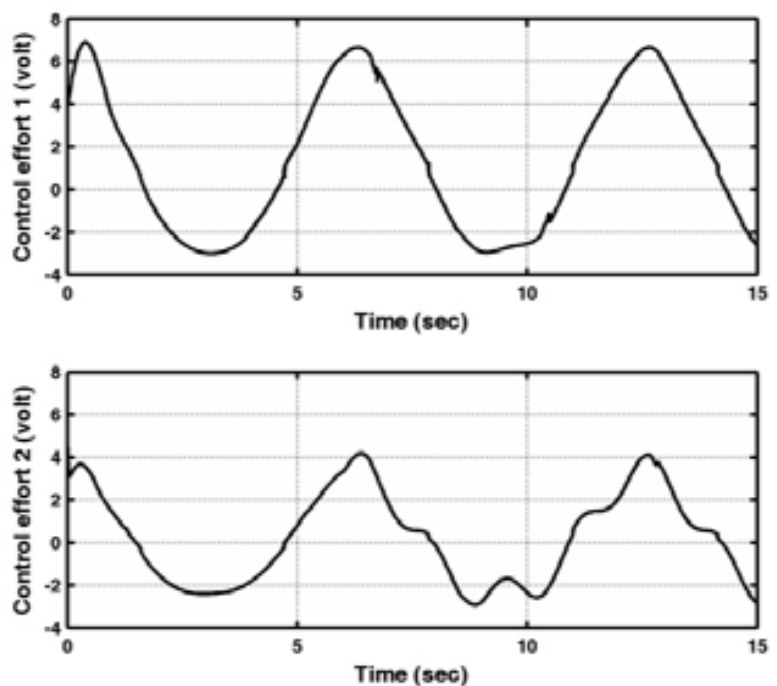


(b)

Fig. 26. (sim2) Tracking error of joints (a) FSM\_PID (b) NNSM\_PID



(a)



(b)

Fig. 27. (sim2) Control commands (a) FSM\_PID (b) NNSM\_PID

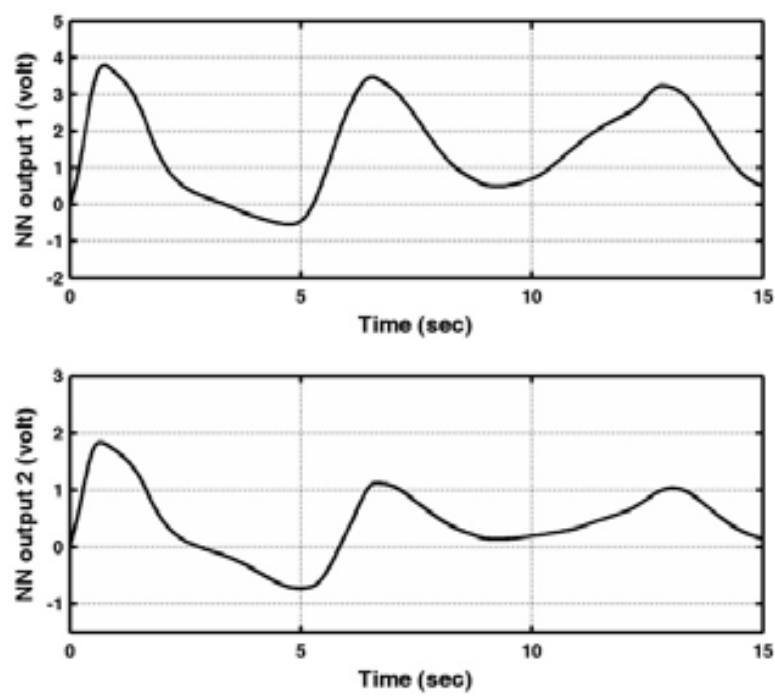


Fig. 28. (sim2) NN control effort

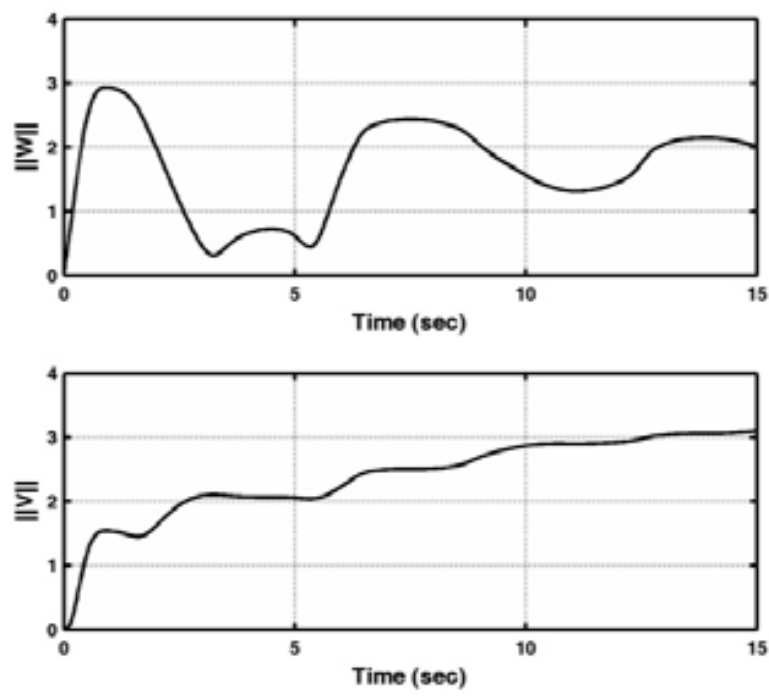


Fig. 29. (sim2) Matrix norm of adaptive weights  $\|W\|$  and  $\|V\|$



#### 4. Conclusion

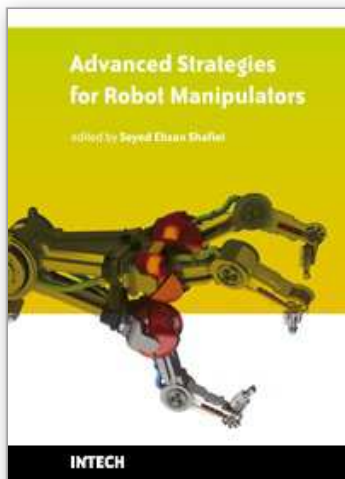
This chapter addressed sliding mode control (SMC) of n-link robot manipulators by using of intelligent methods including fuzzy logic and neural network strategies. In this regard, three control strategies were investigated. In the first case, design of a sliding mode control with a PID loop for robot manipulator was presented in which the gain of both SMC and PID was tuned on-line by using fuzzy approach. The proposed methodology in fact tries to use the advantages of the SMC, PID and Fuzzy controllers simultaneously, i. e., the robustness against the model uncertainty and external disturbances, quick response, and on-line automatic gain tuning, respectively. Finally, the simulation results of applying the proposed methodology to a two-link robot were provided and compared with corresponding results of the conventional SMC which show the improvements of results in the case of using the proposed method. In the second case, a new combination of sliding mode control and fuzzy control is proposed which is called incorporating sliding mode and fuzzy controller. Three practical aspects of robot manipulator control are considered there, such as restriction on input torque magnitude due to saturation of actuators, friction and modeling uncertainty. In spite of these features, the designed controller can improve the sliding mode and fuzzy controller performance in the tracking error and faster transient points of view, respectively. As previous case, the simulation results of applying the proposed methodology and other two methodologies to a two-link direct drive robot arm were provided. Comparing these results demonstrate the success of the proposed method.

Whenever, fast and high-precision position control is required for a system which has high nonlinearity and unknown parameters, and also, suffers from uncertainties and disturbances, such as robot manipulators, in that case, necessity of designing a developed controller that is robust and has self-learning ability is appeared. For this purpose, an efficient combination of sliding mode control, PID control and neural network control for position tracking of robot manipulators driven by permanent magnet DC motors was addressed in the third case. SMC is robust against uncertainties, but it is extremely dependent on model and uses unnecessary high control gain; So, NN control approach is employed to approximate major part of the model. A PID part was added to make the response faster, and to assure the reaching of sliding surface during initial period of weight adaptations. Moreover, four practical aspects of robot manipulator control such as actuator dynamics, restriction on input armature voltage of actuators due to saturation of them, friction and uncertainties were considered. In spite of these features, the controller was designed based on Lyapunov stability theory and it could carry out the position control with fast transient and high-precision response, successfully. Finally, two-step simulation was performed and its results confirmed the success of presented approach. However, the presented design was performed in the joint space of robot manipulator and kinematic uncertainty was not considered. For the future work, one can expand this method to work space design with uncertain kinematics.

#### 5. References

- Ataei, M. & Shafiei, S. E. (2008). Sliding Mode PID Controller Design for Robot Manipulators by Using Fuzzy Tuning Approach, *Proceedings of the 27<sup>th</sup> Chinese Control Conference*, July 16-18 2008, Kunming, Yunnan, China, pp. 170-174.
- Cai, L. & Song, G. (1994). Joint Stick-Slip Friction Compensation of Robot Manipulators by using Smooth Robust Controllers, *Jurnal of Robotic Systems*, Vol. 11, No. 6, pp. 451-470.

- Calcev, G. (1998). Some Remarks on the Stability of Mamdani Fuzzy Control Systems, *IEEE Transactions on Fuzzy Systems*, Vol. 6, No. 4., pp. 436-442.
- Capisani, L. M.; Ferrara, A. & Magnani, L. (2009). Design and experimental validation of a second-order sliding-mode motion controller for robot manipulators, *International Journal of Control*, vol. 82, no. 2, pp. 365-377.
- Chang, Y. C.; Yen, H. M. & Wu, M. F. (2008). An intelligent robust tracking control for electrically driven robot systems, *International Journal of Systems Science*, vol. 39, no. 5, pp. 497-511.
- Chang, Y. C. & Yen, H. M. (2009). Robust tracking control for a class of uncertain electrically driven robots, *IET Control Theory and Applications*, vol. 3, no. 5, pp. 519-532.
- Craig, J. J. (1986). *Introduction to Robotics*, Addison& Wesley, Inc.
- Eker, I. (2006). Sliding mode control with PID sliding surface and experimental application to an electromechanical plant, *ISA Transaction.*, vol. 45, no. 1, pp. 109-118.
- Hung, J. Y.; Gao, W. & Hung, J. C. (1993). Variable structure control: A survey, *IEEE Transactions on Industrial Electronics*, vol. 40, pp. 2-21.
- Kaynak, O.; Erbatur, K. & Ertuğrul, M. (2001). The Fusion of Computationally Intelligent Methodologies and Sliding-Mode Control: A Survey, *IEEE Transactions on Industrial Electronics*, vol. 48, no. 1, pp. 4-17.
- Khalil, K. H. (2001). *Nonlinear Systems*, Third edition, Prentice Hall Inc, New York, USA.
- Lee, C. C. (1990). Fuzzy Logic in Control Systems: Fuzzy Logic Controller-Part I and II, *IEEE Transaction on System, Man and Cybernetics*, Vol. 20, No. 2, 404-435.
- Lewis, F. L.; Yesidirek, A. & Liu, K. (1996). Multilayer Neural-Net Robot Controller with Guaranteed Tracking Performance, *IEEE Transactions on Neural Networks*, vol. 7, no. 2.
- Lewis, F. L.; Jagannathan, S. & Yesildirek, A. (1998). *Neural Network Control of Robot Manipulators and Nonlinear Systems*, Taylor & Francis.
- Santibanez, V.; Kelly, R. & Liama, L.A. (2005). A Novel Global Asymptotic Stable Set-Point Fuzzy Controller with Bounded Torques for Robot Manipulators, *IEEE Transactions on Fuzzy Systems*, Vol. 13, No. 3, pp. 362-372.
- Shafiei, S. E. & Sepasi, S. (2010). Incorporating Sliding Mode and Fuzzy Controller with Bounded Torques for Set-Point Tracking of Robot Manipulators, Scheduled for publishing in the *Journal of Electronics and Electrical Engineering, T125 Automation, Robotics*, No. 10(106).
- Shafiei, S. E. & Soltanpour, M. R. (2010). Neural Network Sliding-Model-PID Controller Design for Electrically Driven Robot Manipulators, Scheduled for publishing in the *International journal of Innovative Computing, Information and Control*, vol. 6, No. 12.
- Slotin, J. J. E. & Li, W. (1991). *Applied Nonlinear Control*. Englewood Cliffs, NJ: Prentice-Hall, New York, USA.
- Spong, M. W. & Vidyasagar, M. (1989) *Robot Dynamics and Control*, Wiley, New York, USA.
- Utkin, V. I. (1978). *Sliding Modes and their Application in Variable Structure Systems*, MIR Publishers, Moscow.
- Wai, R. J. & Chen, P. C. (2006). Robust Neural-Fuzzy-Network Control for Robot Manipulator Including Actuator Dynamics, *IEEE Transactions on Industrial Electronics*, vol. 53, no. 4, pp. 1328-1349.
- Wang, L. X. (1997). *A Course in Fuzzy Systems and Control*, Prentice Hall, NJ, New York, USA.
- Zhang, M.; Yu, Z.; Huan, H. & Zhou, Y. (2008). The Sliding Mode Variable Structure Control Based on Composite Reaching Law of Active Magnetic Bearing, *ICIC Express Letters*, vol.2, no.1, pp.59-63.



## **Advanced Strategies for Robot Manipulators**

Edited by S. Ehsan Shafiei

ISBN 978-953-307-099-5

Hard cover, 428 pages

**Publisher** Sciyo

**Published online** 12, August, 2010

**Published in print edition** August, 2010

Amongst the robotic systems, robot manipulators have proven themselves to be of increasing importance and are widely adopted to substitute for human in repetitive and/or hazardous tasks. Modern manipulators are designed complicatedly and need to do more precise, crucial and critical tasks. So, the simple traditional control methods cannot be efficient, and advanced control strategies with considering special constraints are needed to establish. In spite of the fact that groundbreaking researches have been carried out in this realm until now, there are still many novel aspects which have to be explored.

### **How to reference**

In order to correctly reference this scholarly work, feel free to copy and paste the following:

S. Ehsan Shafiei (2010). Sliding Mode Control of Robot Manipulators via Intelligent Approaches, Advanced Strategies for Robot Manipulators, S. Ehsan Shafiei (Ed.), ISBN: 978-953-307-099-5, InTech, Available from: <http://www.intechopen.com/books/advanced-strategies-for-robot-manipulators/sliding-mode-control-of-robot-manipulators-via-intelligent-approaches>

**INTECH**  
open science | open minds

### **InTech Europe**

University Campus STeP Ri  
Slavka Krautzeka 83/A  
51000 Rijeka, Croatia  
Phone: +385 (51) 770 447  
Fax: +385 (51) 686 166  
[www.intechopen.com](http://www.intechopen.com)

### **InTech China**

Unit 405, Office Block, Hotel Equatorial Shanghai  
No.65, Yan An Road (West), Shanghai, 200040, China  
中国上海市延安西路65号上海国际贵都大饭店办公楼405单元  
Phone: +86-21-62489820  
Fax: +86-21-62489821

© 2010 The Author(s). Licensee IntechOpen. This chapter is distributed under the terms of the [Creative Commons Attribution-NonCommercial-ShareAlike-3.0 License](https://creativecommons.org/licenses/by-nc-sa/3.0/), which permits use, distribution and reproduction for non-commercial purposes, provided the original is properly cited and derivative works building on this content are distributed under the same license.

IntechOpen

IntechOpen